

RESEARCH

Open Access



Changes of intestinal microbiome and its relationship with painful diabetic neuropathy in rats

Shuaiying Jia¹, Haiqi Mi¹, Yao Su¹, Yuning Liu¹, Zhi Ming¹ and Jingyan Lin^{1*}

Abstract

Objective To analyze the gut bacterial microbiome in rats with painful diabetic neuropathy (PDN) compared to normal rats.

Methods Type 2 diabetes was induced in rats via a high-fat and high-sugar diet combined with a low dose of streptozotocin. Glucose metabolism and insulin sensitivity were evaluated using intraperitoneal glucose tolerance tests and insulin tolerance tests. The progression of peripheral neuropathy was assessed using the mechanical withdrawal threshold and thermal withdrawal latency. Histopathological analysis of rat colon tissues was performed using hematoxylin–eosin staining to observe morphological changes. The expression levels of pro-inflammatory cytokines TNF- α and IL-1 β in spinal cord tissues were measured using enzyme-linked immunosorbent assay (ELISA). Fecal samples were then collected for metagenomic sequencing and analysis.

Result Behavioral tests revealed reduced mechanical withdrawal threshold and thermal withdrawal latency in PDN rats. Histological analysis showed significant colonic mucosal damage and inflammatory cell infiltration, suggesting impaired intestinal barrier function. Elevated TNF- α and IL-1 β levels in spinal cord tissues further highlight peripheral inflammation's role in PDN. Sequencing analysis revealed significant differences in gut microbiota composition between PDN and control rats, with altered Bacillota/Bacteroidota ratios and increased Lactobacillus abundance. Functional annotation analysis, based on the KEGG, EggNOG, and CAZy databases, indicated significant enrichment of metabolic pathways related to carbohydrate and amino acid metabolism, energy metabolism, and cell structure biogenesis in PDN rats. Cluster analysis identified higher functional clustering in Metabolism and Genetic Information Processing pathways in PDN rats.

Conclusion This study demonstrates that PDN leads to altered gut microbiota composition, disrupted metabolic pathways, and increased inflammation, contributing to the pathological progression of diabetic neuropathy. This study provides new insights into the interplay between gut microbiota and diabetic neuropathy, offering potential avenues for therapeutic interventions targeting microbiome and metabolism.

Keywords Painful diabetic neuropathy, Gut microbiota, Fecal metagenomic sequencing, Neuropathic pain, Lactobacillus, Collinsella

*Correspondence:

Jingyan Lin
linjingyan@nsmc.edu.cn

¹ Department of Anesthesiology, The Affiliated Hospital of North Sichuan Medical College, 234 Fujiang Road, Shunqing District, Nanchong, Sichuan 637000, China



© The Author(s) 2025. **Open Access** This article is licensed under a Creative Commons Attribution-NonCommercial-NoDerivatives 4.0 International License, which permits any non-commercial use, sharing, distribution and reproduction in any medium or format, as long as you give appropriate credit to the original author(s) and the source, provide a link to the Creative Commons licence, and indicate if you modified the licensed material. You do not have permission under this licence to share adapted material derived from this article or parts of it. The images or other third party material in this article are included in the article's Creative Commons licence, unless indicated otherwise in a credit line to the material. If material is not included in the article's Creative Commons licence and your intended use is not permitted by statutory regulation or exceeds the permitted use, you will need to obtain permission directly from the copyright holder. To view a copy of this licence, visit <http://creativecommons.org/licenses/by-nc-nd/4.0/>.

Background

With the annual increase in the global number of diabetes patients, the type 2 diabetes mellitus (T2DM) has become one of the most serious global epidemics of the twenty-first century [1]. According to statistics, the global prevalence of T2DM has escalated to epidemic levels, currently affecting an estimated population exceeding 400 million individuals worldwide [2]. Among these, nearly half experience varying degrees of neuropathic pain caused by damage to the peripheral or autonomic nervous systems. Painful diabetic neuropathy (PDN), the most common type, accounts for approximately 75% of all neuropathies [3]. Typical symptoms of PDN include symmetrical burning sensations, electric shock-like pain, and tingling in both hands and/or lower limbs, which may or may not be accompanied by numbness. These symptoms significantly reduce patients' quality of life and may lead to anxiety, depression, and sleep disturbances, potentially resulting in disability in severe cases [4, 5]. Currently, the treatment efficacy for PDN is often unsatisfactory; common pharmacological therapies include antidepressants, anticonvulsants, and analgesics, yet these treatments are frequently limited in effectiveness and may have adverse side effects [6]. Therefore, it is imperative to investigate the underlying mechanisms of PDN and identify new therapeutic targets.

However, the pathogenesis of PDN is complex, involving various factors such as glycemic control, the duration of diabetes, patient age, blood pressure, lipid levels, and body weight [7]. Additionally, biochemical processes like increased free radicals [8], the formation of advanced glycation end-products [9], and endoplasmic reticulum stress [10] also play significant roles in the occurrence and progression of PDN. Recent studies have further revealed the potential involvement of μ -opioid receptors and μ - δ opioid receptor heteromers in neuropathic pain. Specifically, spinal nerve injury may promote the increased μ - δ heterodimerization in uninjured dorsal root ganglion neurons, suggesting that μ - δ heteromers could be a potential therapeutic target for alleviating neuropathic pain [11]. Furthermore, the activation of peripheral μ -opioid receptors has been shown to effectively alleviate behavioral and neurobiological abnormalities in a chemotherapy-induced neuropathic pain rat model [12]. This suggests that opioid receptors may also have a potential therapeutic role in PDN. At the same time, nanomedicine, as an emerging therapeutic strategy, has demonstrated unique advantages in the treatment of neuropathic pain. By combining nanoparticle drugs, cell therapy, and gene therapy, nanomedicine holds promise in improving therapeutic efficacy while reducing side effects. However, the application of nanomedicine in neuropathic pain treatment still faces several

challenges, including the development of well-characterized nanoparticle formulations, ensuring batch-to-batch reproducibility, and controlling toxicity [13]. Therefore, further exploration and optimization of nanomedicine are needed for its future application in PDN treatment. Additionally, Our previous studies have suggested that the distribution and expression of Aquaporin-4 in the spinal cord glial lymphatic system may be associated with the pathogenesis of PDN [14, 15]. Nonetheless, the complete mechanisms underlying PDN remain to be fully elucidated. Despite these insights, the full understanding of the pathogenesis of PDN remains elusive. Future research will continue to explore the interactions of various molecular mechanisms and their impact on the development of PDN.

In recent years, the role of gut microbiota in various metabolic diseases has gained increasing attention. Moreover, changes in the composition of gut microbiota are closely linked to the onset of diabetes and its complications [16, 17]. Specifically, gut microbiota in diabetes patients typically exhibit reduced diversity, a decrease in beneficial bacterial species (such as probiotics), and an increase in potentially harmful bacterial species [18]. These alterations may influence the functioning of the nervous system through various mechanisms, including altered short-chain fatty acid (SCFA) metabolism, interactions with gut hormones, increased production of trimethylamine-N-oxide, bacterial translocation, and endotoxin production such as lipopolysaccharide [16]. These factors have been shown to significantly impact the nervous system and are closely related to the occurrence and development of diabetic neuropathic pain.

Studies have shown that, compared to diabetic patients without neuropathy and healthy individuals, patients with diabetic neuropathy exhibit a decrease in the abundance of *Bacteroides* and *Faecalibacterium*, while the quantities of *Escherichia-Shigella*, *Lachnoclostridium*, *Blautia*, *Megasphaera*, and *Ruminococcus torques* significantly increase. Further investigations have suggested that these microbial changes may be associated with insulin resistance, indicating a close relationship between the presence of insulin resistance and the onset of diabetic neuropathy [19]. Additionally, studies have found that modulating the gut microbiota, such as through the administration of *Bifidobacterium*, *Lactobacillus*, or fecal microbiota transplantation, can improve insulin resistance [20]. Moreover, the gut microbiota, through its metabolic products, may directly influence the nervous system. For example, toxins produced by certain bacteria can activate pain receptors, thereby contributing to chronic pain [21, 22]. A clinical study has shown that the abundance of *Parabacteroidetes* in the gut microbiota of patients with diabetic neuropathy is correlated with

changes in C-reactive protein (CRP) and bile acid salts levels [19]. These findings further suggest that the gut microbiota may play an important role in the development of diabetic neuropathy. Given the regulatory effects of the gut microbiota on insulin resistance and its potential impact on diabetic neuropathy, investigating how the gut microbiota participates in the pathogenesis of PDN could provide new directions for early diagnosis, treatment, and personalized medicine for PDN.

This study aims to investigate the relationship between changes in gut microbiota and diabetic neuropathic pain in a rat model. By comparing gut microbiome data from healthy and diabetic rats, we hope to uncover the potential impact of gut microbiota alterations on the pathogenesis of PDN. This research not only provides new insights into the understanding of diabetes and its complications but may also lay the groundwork for developing novel therapeutic strategies to improve the quality of life and prognosis for diabetes patients.

Methods

PDN model establishment and animal grouping

This experiment involved 25 male Sprague–Dawley rats, aged 6–8 weeks and weighing 180–200 g, provided by the Experimental Animal Center of North Sichuan Medical College. The rats were housed in a specific pathogen-free laboratory, where the environmental conditions were maintained at a temperature of 23 ± 2 °C, humidity of 40%–70%, and a 12-h light/dark cycle, with free access to food and water. Standard maintenance diet was provided by the Experimental Animal Center, while the high-fat and high-sugar diet was purchased from Xiaoshuyoutai (Beijing) Biotechnology Co., LTD., catalog number D12450 J (including 5% cholesterol, 10% lard, and 10% sucrose). All experimental procedures were approved by the Institutional Ethics Committee of North Sichuan Medical College (authorization number: 2024[071]). All procedures adhered strictly to the ARRIVE guidelines for the Care and Use of Experimental Animals.

The rats were randomly divided into two groups: group control (group C, $n = 5$) and group model (group M, $n = 20$). After one week of acclimatization, the group C continued to receive a standard maintenance diet, while the group M was fed a high-fat, high-sugar diet. Continued feeding for 4 weeks. During this period, body weight and blood glucose levels were measured weekly for both groups. In the fifth week, the rats of group M were fasted for 10 h before being administered a single intraperitoneal injection of streptozotocin (STZ, purchased from Efa Biological Company, Lot: MRDD2303) at a dose of 25 mg/kg, dissolved in a sodium citrate solution (0.1 mol/L, pH 4.5). The group C received an equal volume of sodium citrate buffer. Three days post-injection, fasting blood

glucose levels were reassessed; a level of ≥ 16.7 mmol/L was considered indicative of successful induction. Rats not meeting this criterion received a second injection at the same dosage. Following two injections, a total of 17 rats exhibited elevated blood glucose levels.

After successfully inducing hyperglycemia in the rats, all animals were fed a standard maintenance diet. Subsequently, we continuously monitored the 24-h water and food intake of both groups of rats over the following week, randomly selecting data from days 1, 4, and 7 for statistical analysis. Based on the statistical results and dynamic observations, we adjusted the daily food intake of both groups to 30 g per 100 g of body weight (30 g/100 g body weight). Thereafter, during the entire experimental period, food was precisely weighed using an electronic scale and administered in fixed amounts daily until the conclusion of the experiment. Additionally, regular assessments of mechanical allodynia and thermal hyperalgesia were conducted in the group C ($n = 5$) and group M ($n = 17$) of rats to evaluate the extent of peripheral nerve injury. In the 15th week of the experiment, the group C and the group M of rats underwent intraperitoneal glucose tolerance tests and insulin tolerance tests to assess glucose metabolism and insulin sensitivity. A total of 10 rats (5 from the group C and 5 from the group PDN) were ultimately included in the experiments. The remaining rats were excluded due to insufficient blood glucose levels, minimal peripheral nerve damage, low degrees of insulin resistance, or other complications. All excluded rats were euthanized in accordance with ethical guidelines.

Intraperitoneal glucose tolerance and insulin tolerance experiments

Intraperitoneal glucose tolerance test (IPGTT)

In the 15th week of the experiment, five rats each from the PDN group and the healthy control group were selected to undergo an IPGTT. The rats were fasted for 12 h with free access to water, after which fasting blood glucose was measured to establish a baseline. Following this, a 50% glucose solution was administered intraperitoneally at a dose of 2 g/kg, and blood glucose levels were measured at 30 min, 60 min, 90 min, and 120 min post-injection [23].

Insulin tolerance test (ITT)

Forty-eight hours after the completion of the IPGTT, a total of 10 rats from both the group PDN and group C underwent an ITT. In this experiment, regular insulin (NovoRapid, Novo Nordisk, Denmark) was administered intraperitoneally at a dose of 0.5 U/kg. Baseline blood

glucose levels were measured prior to the injection, followed by measurements at 30 min, 60 min, 90 min, and 120 min post-injection. The evaluation of ITT was based on the percentage change in serum glucose relative to baseline levels [24].

Mechanical allodynia and thermal hyperalgesia

Mechanical allodynia

Mechanical allodynia was assessed through the mechanical withdrawal threshold (MWT). Beginning in the sixth week of the experiment, a trained experimenter evaluated the MWT of the rats' hind paws using a Von Frey filament apparatus (U.S. Patent No. 58239698512259, North Coast, CA, United States). These assessments were conducted weekly, between 9 and 11 AM, in a quiet environment. Specifically, each rat was placed on a mesh metal platform for 15 min to acclimate and remain relaxed. Subsequently, von Frey filaments were used to stimulate the area between the third and fourth metatarsal bones of the hind paw, starting at a force of 0.2 g and increasing until the rat either withdrew its paw or licked it (paw withdrawal threshold to pressure). Each application of pressure lasted for 5 s, with tests alternating every 2 min. A positive withdrawal response in three out of five consecutive trials was recorded as the MWT, with the final MWT determined as the average of three stable consecutive measurements, expressed in grams. To prevent paw injury and ensure compliance with equipment specifications, the maximum strength of the Von Frey filaments was limited to 26 g [25].

Thermal hyperalgesia

Thermal hyperalgesia is assessed by measuring the thermal withdrawal latency (TWL) in rats. For the procedure, individual rats are first placed in transparent, square, glass enclosures with removable floors (dimensions: 22 × 12 × 22 cm) to acclimatize for 15 min. Following this adaptation period, a thermal nociception meter (Model: LE7420, Serial No: 1491712, Bioseb, France) is preheated to 55 °C. The glass enclosure is then positioned over the nociception meter, and the floor is removed to expose the rat's hind paws to the heated surface. The timer starts when the plantar surface of the hind paw contacts the heat plate. The timing is halted when the rat displays any nocifensive behaviors such as lifting, licking, or withdrawing the foot. The duration until these responses occur is recorded as the TWL. Each rat undergoes three such trials, with a 5-min interval between each trial to prevent sensitization and thermal injury. The final TWL for each rat is determined by calculating the average of the three measurements. This method ensures a robust assessment of thermal hyperalgesia [26].

Pathological staining

Colon tissues were collected from Sprague–Dawley rats and rinsed with physiological saline to remove surface blood and impurities. The tissues were then fixed in 10% neutral buffered formalin for 24–48 h. Following fixation, the tissues were subjected to dehydration, clearing processes, culminating in paraffin embedding. The embedded tissues were sectioned into 4- μ m thick consecutive slices using a microtome. The sections were floated on a 37 °C water bath to flatten, transferred onto glass slides, and baked in a 60 °C oven for 30 min to ensure adhesion and remove excess paraffin. The sections were deparaffinized with xylene and rehydrated through a graded ethanol series. Hematoxylin staining was performed, followed by differentiation in acid-alcohol (1% HCl in 70% ethanol) and bluing in water. Subsequently, the sections were counterstained with 0.5% eosin solution. After staining, the sections underwent dehydration through graded ethanol, clearing with xylene, and were finally mounted with neutral resin and covered with cover slips. The stained sections were observed under a light microscope, and images were captured to evaluate the morphological structure and pathological changes in the rat colon tissue.

Proinflammatory biomarkers

Spinal cord tissues were collected, weighed, and homogenized in ice-cold phosphate-buffered saline (PBS) supplemented with protease inhibitors to prevent protein degradation. The homogenate was centrifuged at 12,000 ×g for 20 min at 4 °C to remove debris, and the supernatant was collected. The total protein concentration of the supernatant was measured using a bicinchoninic acid (BCA) assay to ensure uniform loading across samples. The concentrations of TNF- α (FineTest, China, ER1393) and IL-1 β (FineTest, China, ER1094) in spinal cord tissue were quantified using commercial ELISA kits, following the manufacturer's instructions. The optical density (OD) was measured at 450 nm using a microplate reader (TeBao, USA) within 30 min of stopping the reaction. The concentration of TNF- α and IL-1 β in each sample was calculated by plotting the OD values against the standard curve prepared with known concentrations of the cytokines. Cytokine concentrations were normalized to the total protein concentration of each sample and expressed as pg/mg of protein. All experiments were performed in triplicate to ensure reproducibility.

Sample collection

In this experiment, all rats were first deeply anesthetized via intraperitoneal injection of 1% pentobarbital sodium at a dosage of 50 mg/kg body weight. Following anesthesia, the colon was rapidly incised using a sterile surgical

scalpel, and the colonic contents were collected with sterile sampling tubes. Once collection was completed, the samples were immediately flash-frozen in liquid nitrogen and subsequently stored at -80°C until further analytical processing.

Extraction and detection of sample DNA

In this study, genomic DNA was extracted from the colon contents of ten rats using the cetyltrimethylammonium bromide (CTAB) method. The specific steps are as follows: 1000 μL of CTAB lysis buffer and an appropriate amount of lysozyme were added to a 2.0 mL centrifuge tube. The colon samples were then added to the lysis buffer and incubated in a water bath at 65°C . During this period, the mixture was gently inverted several times to promote complete lysis of the samples. Next, the samples were centrifuged to obtain the supernatant. The supernatant was mixed with phenol, chloroform, and isoamyl alcohol (in a ratio of 25:24:1), and centrifuged at 12,000 rpm for 10 min. The upper phase was collected and mixed with chloroform and isoamyl alcohol (in a ratio of 24:1), followed by a second centrifugation at 12,000 rpm for 10 min. Subsequently, the supernatant was transferred to a 1.5 mL centrifuge tube, and isopropanol was added to precipitate the DNA, which was then stored at -20°C . After centrifugation, the supernatant was discarded, taking care to retain the precipitate. The precipitate was washed twice with 1 mL of 75% ethanol, and any remaining liquid was collected by centrifugation. Finally, the supernatant was carefully removed, and the precipitate was dried in a sterile workbench or at room temperature. Deionized water (ddH_2O) without enzymes was added to dissolve the DNA sample, and incubation at $55\text{--}60^{\circ}\text{C}$ for 10 min was performed if necessary to facilitate dissolution. Subsequently, 1 μL of RNase A was added to digest RNA and incubated at 37°C for 15 min. Finally, the concentration, integrity, and purity of the DNA were assessed using the Agilent 5400 system.

Library construction and sequencing

After quality assessment, DNA libraries were constructed using the NEBNext[®] Ultra[™] DNA Library Prep Kit for Illumina (NEB, USA, Catalog #: E7370L). The DNA samples were fragmented to approximately 350 bp in length using a Covaris ultrasonic sonicator, followed by end repair, A-tailing, and adapter ligation. Subsequently, fragments were selected, and polymerase chain reaction (PCR) amplification and purification were performed to complete the library preparation. The PCR products were purified using the AMPure XP system (Beverly,

USA), and library quality was evaluated using the Agilent 5400 system. Finally, the library concentration was quantified using quantitative PCR at a concentration of 1.5 nM. Based on the effective library concentration and the required data volume, suitable libraries were selected for high-throughput sequencing on the Illumina platform using the PE150 strategy.

Bioinformatics analysis methods

Metagenomic sequencing of the rat colon contents was performed using the Illumina NovaSeq high-throughput sequencing platform to obtain raw data on microorganisms, including bacteria, fungi, and viruses. To ensure data reliability, the raw sequencing data were preprocessed using the Kneaddata software [27]. In subsequent steps, Kraken2 software was employed to compare the processed sequences against a custom-built microbial nucleic acid database, screening sequences of bacteria, fungi, archaea, and viruses from the NCBI NT nucleotide database and the RefSeq genome database to calculate the sequence counts of species present in the samples [28]. The Bracken software was then used to predict the actual relative abundance of species in the samples. Additionally, HUMAnN2 software was utilized to align the quality-controlled and host-depleted sequences with the protein database (UniRef90) based on DIAMOND, retrieving annotation information and relative abundance tables from various functional databases according to the UniRef90 IDs and the correspondence among databases [29]. Based on species abundance and functional abundance tables, abundance clustering analysis, principal coordinate analysis (PCoA), and non-metric multidimensional scaling (NMDS) were conducted. If group information was available during sample clustering analysis, Lefse biomarker analysis and Dunn's test could be performed to explore differences in species composition and functional composition among the samples.

Statistical methods

The results of the experimental data are presented as mean \pm SEM. Comparisons between two groups were performed using student's t-test, while intergroup differences were assessed through one-way analysis of variance (ANOVA). To account for within-subject variability in variables such as body weight, blood glucose and PWT, repeated measures ANOVA was utilized. All statistical tests were conducted with a two-tailed significance level. The analysis of gut microbiota data was carried out using the bioinformatics platform provided by Shenzhen Microeco Tech Co., Ltd. Other datasets were analyzed using GraphPad Prism 8 software. A *p*-value of less than 0.05 was considered statistically significant.

Result

Basic characteristics

Following the injection of STZ, the blood glucose levels in the group PDN increased immediately. Over time, the blood glucose levels in the group PDN remained persistently elevated (exceeding 20 mmol/L), and body weight began to gradually decline starting from week 7 (Fig. 1A, B). The food and water intake of both groups of rats were measured over a 24-h period on days 1, 4, and 7 after the rise in blood glucose. Compared to the group C, the group PDN exhibited a significant increase in both food and water consumption (Fig. 1C, D). Subsequently, an IPGTT and ITT were conducted to assess the impaired glycemic control within the group PDN. After glucose administration, the blood glucose levels in the group PDN increased significantly and remained elevated for 60 min. Furthermore, compared to the group C, the group PDN exhibited more pronounced fluctuations in blood glucose levels following the injection of regular insulin (Fig. 1E, F). These findings indicate that the group PDN developed typical symptoms of polydipsia, polyphagia, and weight loss, which are consistent with the clinical manifestations of diabetes. Notably, the results of the IPGTT and ITT indicate that the group PDN of rats demonstrates lower efficiency in glucose handling. This suggests that greater amounts of insulin may be required to achieve comparable blood glucose control as seen in the group C, which is indicative of insulin resistance.

Mechanical allodynia and thermal hyperalgesia

Mechanical allodynia and thermal hyperalgesia are primarily used to assess the impact of diabetic neuropathy on pain sensitivity in rats, and are critical for researching PDN. Our measurements indicate that the MWT in the group PDN began to decrease one week after STZ injection, stabilizing after the ninth week (Fig. 2A). Mechanical allodynia is a common symptom of PDN. A reduction in the MWT indicates that PDN rats exhibit an abnormal sensitivity to mild mechanical stimuli. This phenomenon is typically associated with peripheral nerve damage or dysfunction, suggesting a significant decrease in the neural system's tolerance to mechanical stimuli in PDN rats, which implies an increased pain sensitivity. Concurrently, the TWL of the group PDN also showed a significant decrease than that of the group C one week after STZ

injection (Fig. 2B). This finding indicates that PDN rats have impaired thermal perception, resulting in an exaggerated response to temperature stimuli. The occurrence of thermal hyperalgesia suggests abnormalities or degeneration of nerve endings, particularly within the peripheral nervous system. These alterations are likely caused by oxidative stress and neuroinflammation induced by prolonged hyperglycemia. These results demonstrate that PDN rats exhibit significant mechanical allodynia and thermal hyperalgesia, reflecting sensory dysfunction of the peripheral nerves. This provides an effective experimental model for studying the mechanisms of pain associated with diabetic neuropathy.

Histological results and proinflammatory biomarkers

The results of Hematoxylin–eosin (HE) staining revealed significant structural damage to the colonic mucosa in group PDN compared to group C. This damage included loss of mucosal integrity and epithelial cell shedding. Additionally, substantial infiltration of inflammatory cells was observed in the colonic tissue, accompanied by notable lymphoid follicle hyperplasia (Fig. 3A). These pathological changes suggest that the intestinal barrier function in group PDN is compromised, potentially contributing to the development of leaky gut syndrome. Moreover, peripheral inflammation is considered one of the major factors underlying PDN and is associated with increased intestinal permeability. To further investigate this link, key inflammatory biomarkers in spinal cord tissue were evaluated. As shown in Fig. 3B, the levels of TNF- α and IL-1 β in the spinal cord of group PDN was significantly elevated compared to the group C. These findings provide further evidence that PDN may induce inflammatory lesions by impairing intestinal barrier function.

Analysis of intestinal microbial diversity

A total of 245,810,241 paired-end reads were generated from the 10 samples following sequencing, yielding 232,492,896 clean tags after alignment and filtering. On average, each sample contained 23,249,290 clean tags (Table 1). From the rarefaction curve (Fig. 4A), it can be observed that the number of detectable features stabilizes after all samples reach a certain sampling depth. In other words, as the sample size increases to a certain

(See figure on next page.)

Fig. 1 Changes in body weight, blood glucose, intraperitoneal glucose tolerance test (IPGTT), and insulin tolerance test (ITT) results in rats. **A** The trend of body weight in Group C ($n = 5$) and Group PDN ($n = 5$) over 15 weeks (measurements taken weekly); **B** The trend of blood glucose levels in Group C ($n = 5$) and Group PDN ($n = 5$) over 15 weeks (measurements taken weekly); **C** Statistics of 24-h food intake after STZ injection (days 1, 4, 7 post-injection, $n = 5$ per group); **D** Statistics of 24-h water intake after STZ injection (days 1, 4, 7 post-injection, $n = 5$ per group); **E** IPGTT results at the 15 th week after STZ injection ($n = 5$ per group); **F** ITT results at the 15 th week after STZ injection ($n = 5$ per group). Data are presented as mean \pm SDs. Compared with the group C, * $P < 0.05$, ** $P < 0.01$, *** $P < 0.001$, **** $P < 0.0001$

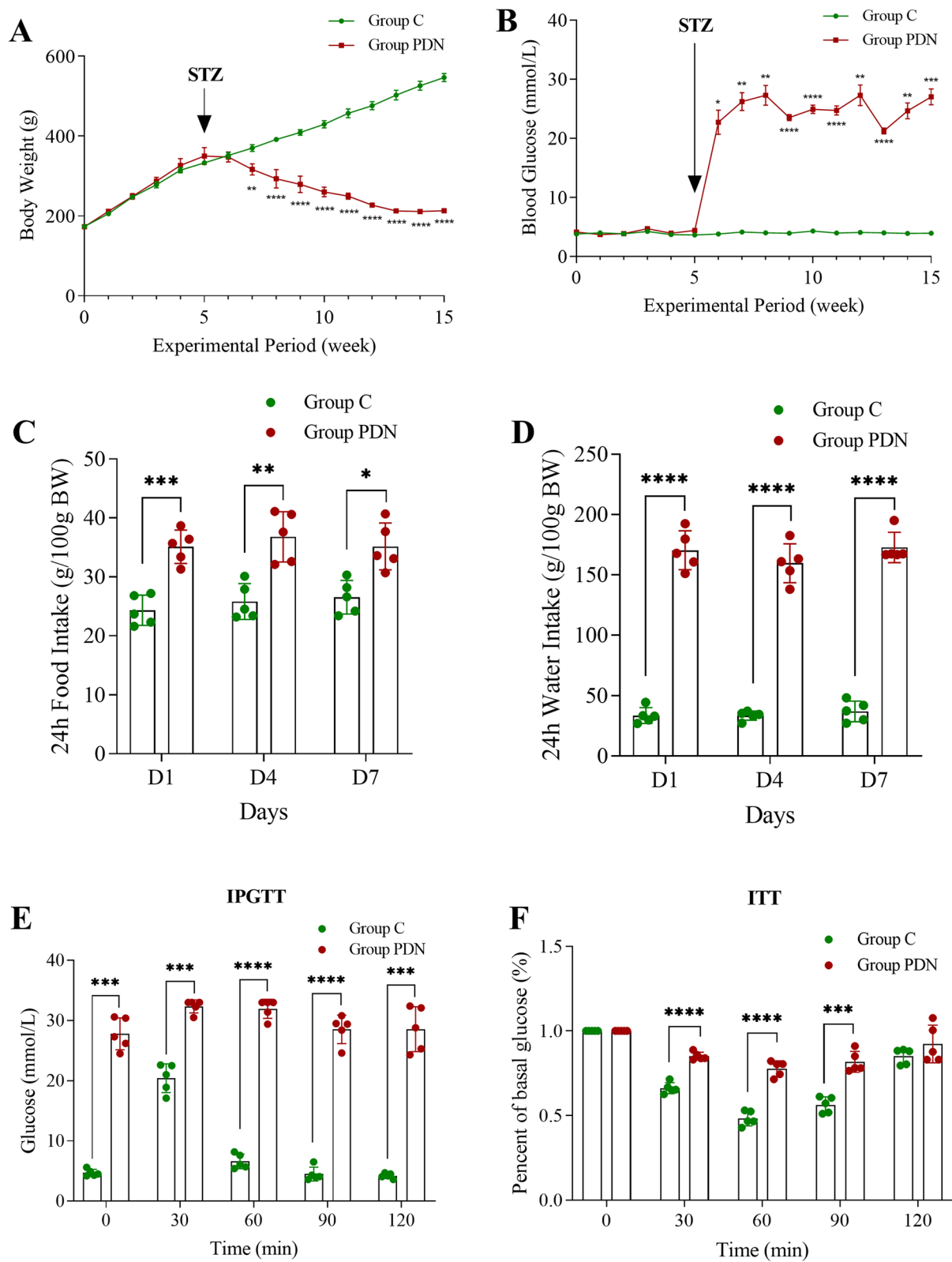


Fig. 1 (See legend on previous page.)

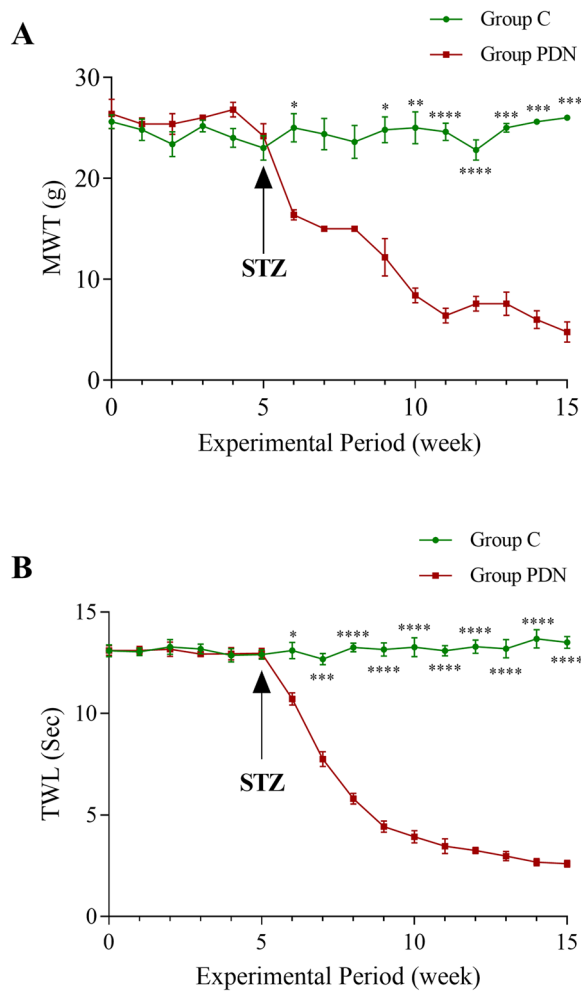


Fig. 2 Evaluation of peripheral neuropathy in rats. **A** The trend of MWT in Group C ($n = 5$) and Group PDN ($n = 5$) over 15 weeks (measurements taken weekly from week 1 to week 15); **B** The trend of TWL in Group C ($n = 10$) and Group PDN ($n = 5$) over 15 weeks (measurements taken weekly from week 1 to week 15). Data are presented as mean \pm SDs. Compared with the group PDN, * $P < 0.05$, ** $P < 0.01$, *** $P < 0.001$, **** $P < 0.0001$

extent, the rate of discovering new features decreases and approaches a plateau. This indicates that the feature richness of the samples used in this study is relatively high or uniformly distributed, making them suitable for bioinformatics analysis. We assessed the diversity of the intestinal microbiota in both groups of rats using α -diversity and β -diversity analyses. The indices used for α -diversity assessment include the coverage index, Chao1 index, Simpson index, and Shannon index. The coverage index reflects the sampling depth of the samples, while the Simpson and Shannon indices are used to measure the diversity and evenness of the communities within the samples. The Chao1 index reflects the richness of the community. As shown in Fig. 4B-E, both groups exhibited similar levels of α -diversity ($P > 0.05$). However, principal coordinates analysis (PCoA) and non-metric multidimensional scaling (NMDS) based on Bray–Curtis dissimilarity demonstrated significant differences in the composition of the intestinal microbial communities between the two groups ($P = 0.022$, $P = 0.021$, Fig. 4F, G). This implies that although there are no significant differences in species richness and evenness between the two groups of rats, their microbial community structures differ significantly. In other words, this may indicate that environmental factors, diet, or other variables have led to differences in community structure.

Analysis of intestinal microbial composition in two groups of rats

Statistical analysis of the species abundance table revealed significant differences in the intestinal microbiota between the group PDN and the group C (Fig. 5A). In this study, we analyzed the top ten phyla of gut microbiota in group PDN and group C. The dominant phyla in both groups were Bacillota, Bacteroidota, Pseudomonadota, and Actinomycetota, collectively accounting for over 85% of the total abundance (Fig. 5D). Compared to the group C, the ratio of

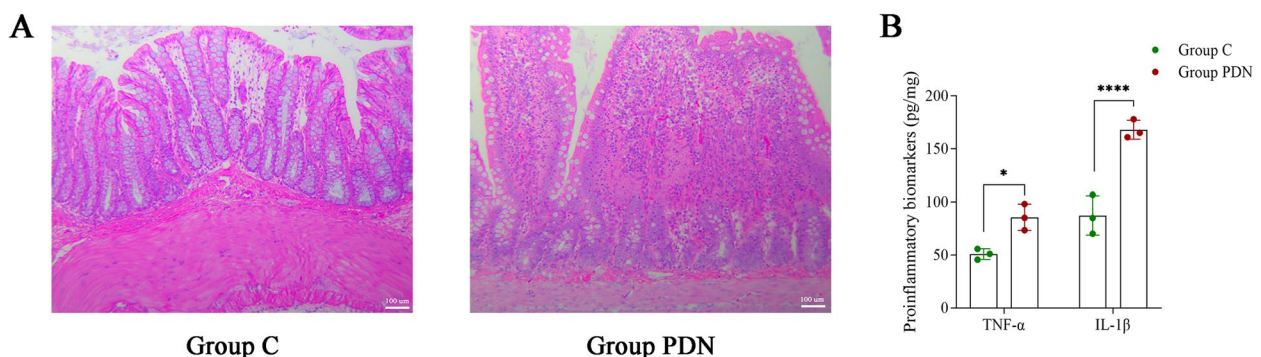


Fig. 3 Pathological changes and Detection of Inflammatory Factors. **A** The HE staining of colonic tissue (x200). Representative images from Group C and Group PDN are shown, Scale bar: 100 μ m; **B** The content of pro-inflammatory cytokines TNF- α and IL-1 β in spinal cord tissue. Values were presented as mean \pm SDs. Compared to the group PDN, * $P < 0.05$, **** $P < 0.0001$

Table 1 The sequences information of fecal samples

Group	Sample ID	Insert size (bp)	Seq strategy	Raw reads (#)	Raw base(GB)	%GC	Raw Q20(%)	Raw Q30(%)	Clean reads (#)	Cleaned (%)	Clean Q20(%)	Clean Q30(%)
C	sample06	350	(150:150)	25332384	7.60	46	98.94	96.71	23881537	94.27	99.50	98.04
C	sample07	350	(150:150)	22318964	6.70	43	98.60	95.66	20232565	90.65	99.41	97.64
C	sample08	350	(150:150)	22208130	6.66	47	98.99	96.78	21306543	95.94	99.49	98.02
C	sample09	350	(150:150)	27048328	8.11	47	98.93	96.66	25929266	95.86	99.48	97.98
C	sample10	350	(150:150)	23483734	7.05	46	98.95	96.70	22482797	95.74	99.48	97.99
PDN	sample11	350	(150:150)	23956733	7.19	46	98.87	96.43	22711541	94.80	99.48	97.94
PDN	sample12	350	(150:150)	22804339	6.84	41	98.66	95.83	20852234	91.44	99.34	97.54
PDN	sample13	350	(150:150)	23876928	7.16	45	98.93	96.59	22865452	95.76	99.47	97.92
PDN	sample14	350	(150:150)	30532576	9.16	49	98.94	96.67	29076088	95.23	99.48	97.96
PDN	sample15	350	(150:150)	24248125	7.27	49	98.90	96.53	23154873	95.49	99.47	97.91

Sample ID: Sample name; Insert Size (bp): The insert size refers to the length chosen during library preparation when cutting the gel. An appropriate insert size can prevent contamination from sequencing adapters; Seq Strategy: Sequencing strategy (typically paired-end, each 150 bp); Raw Reads (#): The number of raw reads obtained from sequencing; Raw Base (GB): The total base number of raw reads, expressed in gigabytes (GB). It is calculated by multiplying the raw reads count by the sequencing length; %GC: The percentage of G/C bases relative to the total number of bases; Clean Reads (#): The number of clean reads obtained after filtering (quality control and removal of host sequences); Cleaned (%): The percentage of remaining sequences after filtering, relative to the total raw reads; Q20: The percentage of bases with a quality score greater than 20; Q30: The percentage of bases with a quality score greater than 30.

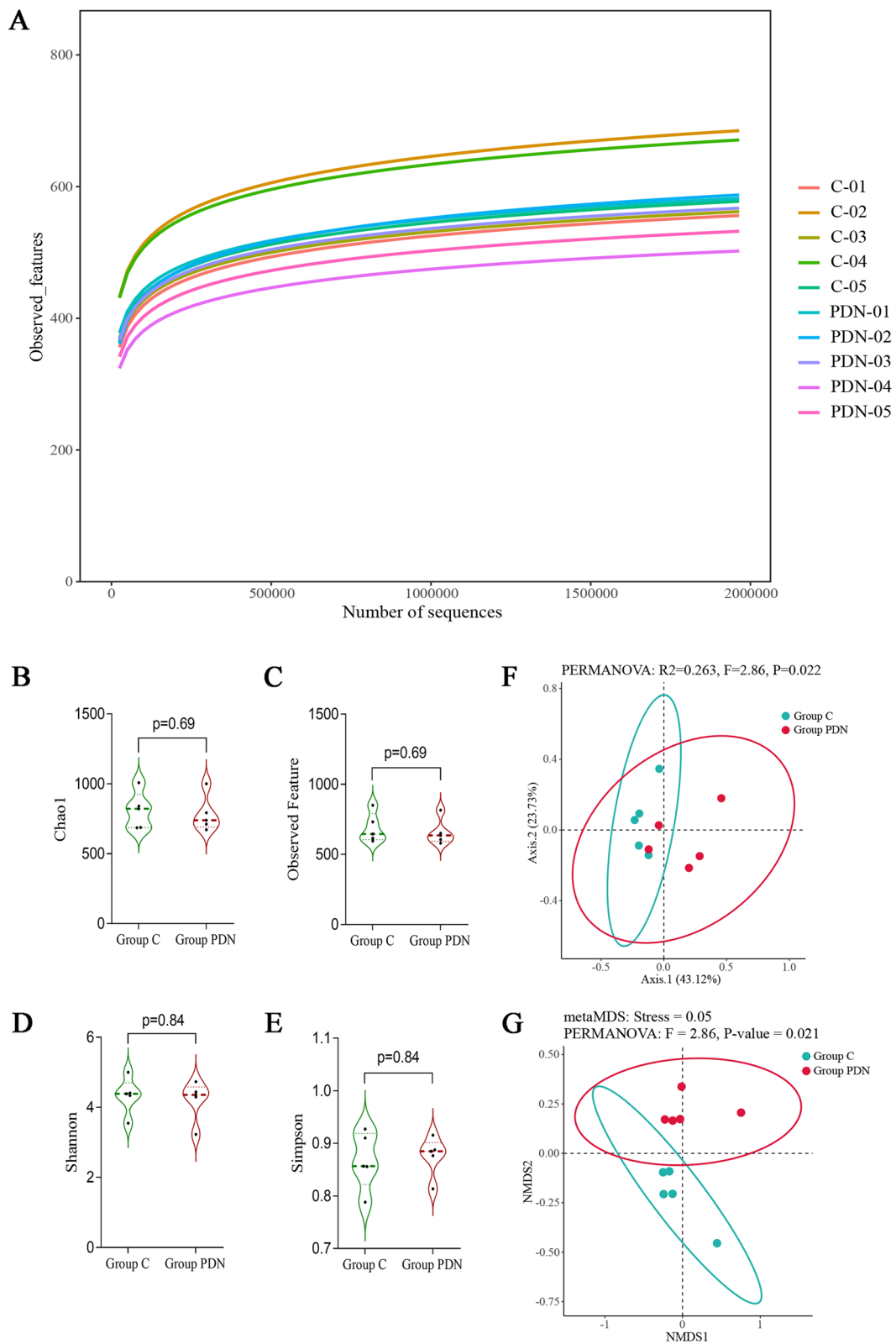


Fig. 4 Analysis of intestinal flora diversity in group C and group PDN. **A-E** Bacterial alpha diversity analysis. **F-G** Bacterial beta diversity analysis. Group C, $n=5$; Group PDN, $n=5$

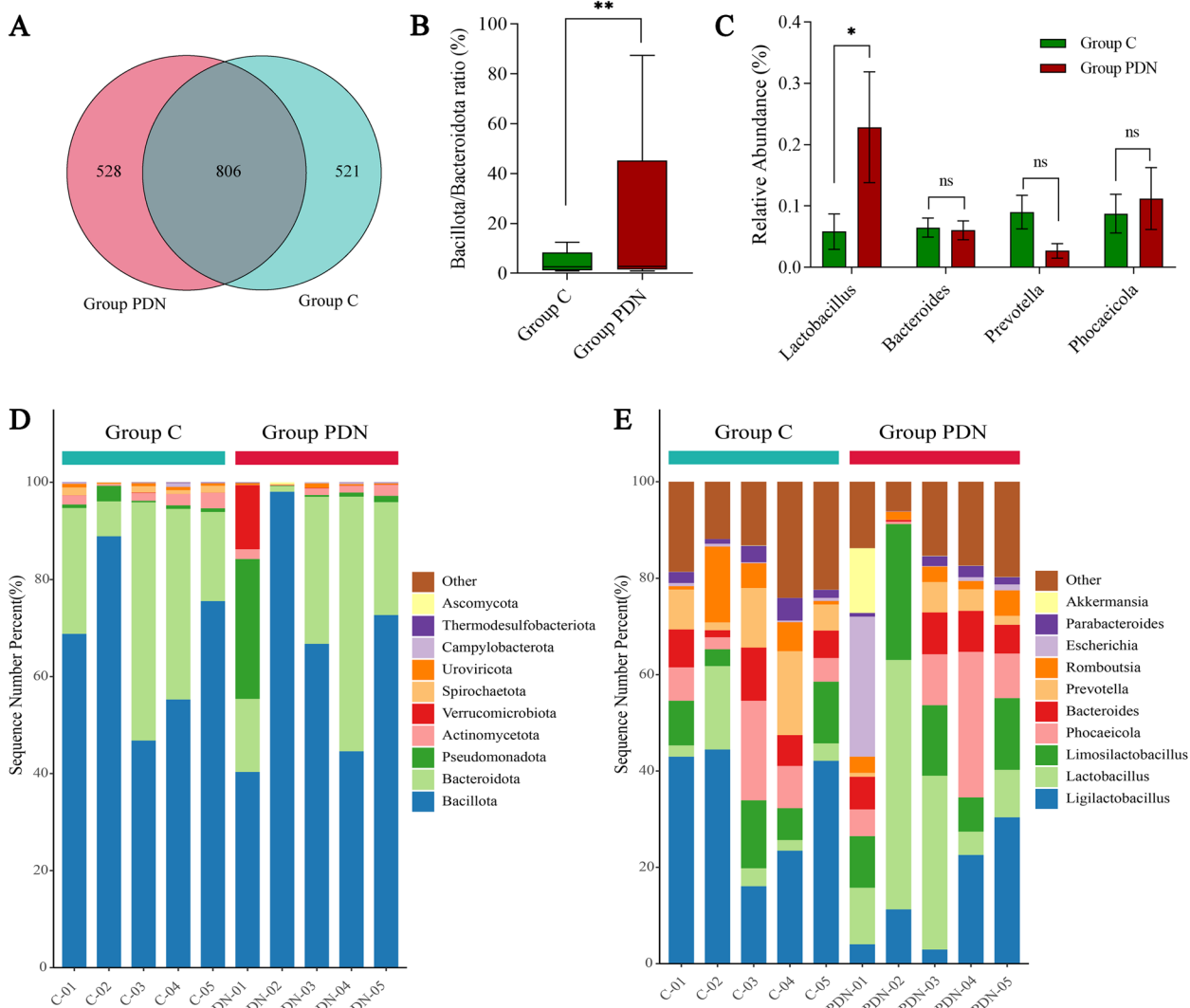


Fig. 5 Relative abundance of species statistical figure (group). **A** Clustering of intestinal flora OTUs in each group of rats Venn diagram. **B** Statistical analysis of the Bacillota/Bacteroidota ratio in the group C and the group PDN. **C** Statistical analysis of bacteria at the genus level that may be associated with the pathogenesis of PDN in the group C and the group PDN. **D** Histogram of relative abundance of species at the phylum level. **E** Histogram of relative abundance of species at the genus level

Bacillotas to Bacteroidetes was significantly increased in the group PDN (Fig. 5B, $P < 0.01$). At the genus level, we similarly analyzed the top ten genera, identifying Ligilactobacillus, Lactobacillus, Limosilactobacillus, and Phocaeicola as dominant genera, together comprising over 50% of the total microbial composition (Fig. 5E). Further analysis revealed an increase in the abundance of Lactobacillus and Phocaeicola in the group PDN, while the abundance of Prevotella decreased (Fig. 5C). This indicates that the gut microbiota structure in the group PDN has undergone alterations. Several studies have indicated that an imbalance in the Bacillota/Bacteroidota ratio is closely associated

with abnormal energy metabolism in T2DM [30, 31]. Our research suggests that the Bacillota/Bacteroidota ratio in the group PDN is significantly higher than that in the group C, which is consistent with existing findings [32]. This indicates that there are abnormalities in energy metabolism in PDN rats.

Analysis of species differences across groups

To screen for species with significant differences in abundance between groups, this study employed the LEfSe (Linear Discriminant Analysis Effect Size) method to compare the gut microbiota of rats in the group C and the group PDN. A threshold for Linear Discriminant

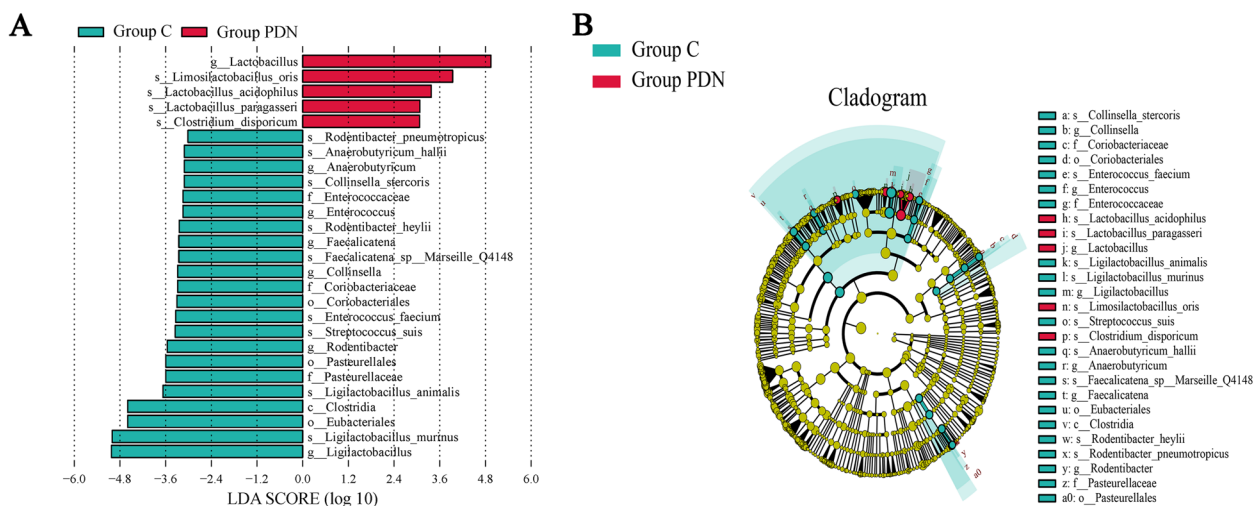


Fig. 6 Analysis of species differences across groups. **A** Histogram of the distribution of LDA values for differing species. **B** Evolutionary branching diagrams for divergent species, circles radiating from inside to outside represent taxonomic levels from phylum to species

Analysis (LDA) was set at 3, and the gut microbiota of the two groups were analyzed from the phylum to species level. As shown in Fig. 6A, there were 27 microbial taxa with significantly different abundances between the two groups; among these, 5 taxa belonged to the group PDN, and 22 belonged to the group C ($LDA > 3, P < 0.05$). It is evident that the genus *Lactobacillus*, the species *Lactobacillus-acidophilus*, *Lactobacillus-paragasseri*, *limosilactobacillus-oris* and *Clostridium-disporicum* were enriched in the group PDN. Furthermore, the class *Collinsella*, the order *Eubacteriales* and *Pasteurellales*, the families *Pasteurellaceae* and *Coriobacteriaceae*, the genera *Ligilactobacillus*, *Rodentibacter*, *Anaerobutyricum*, *Enterococcus* and *Faecalicatena*, the species *Ligilactobacillus-murinus* and *Ligilactobacillus-animalis* were enriched in the group C. Further phylogenetic analysis using a cladogram more comprehensively revealed the specific microbial taxa associated with the onset of PDN (Fig. 6B).

Analysis of relative abundance and differences in the biological functions of rat gut microorganisms

To investigate the potential functional differences in the gut microbiota of two rat groups, we analyzed the data using the KEGG PATHWAY database, the EggNOG database, and the CAZy database.

Analysis of the relative abundance of functional annotations by class

Analysis based on the KEGG PATHWAY database revealed that the most abundant Level 1 metabolic pathways in fecal samples from both rat groups included Metabolism, Genetic Information Processing, and Human Diseases (Fig. 7A). The EggNOG (Evolutionary

Genealogy of Genes: Non-supervised Orthologous Groups) database is a large-scale functional annotation resource used in bioinformatics research, primarily for the functional classification and evolutionary analysis of genes. Analysis using the EggNOG database revealed that functional classes translation (including ribosome assembly and protein folding); replication, recombination, and repair; carbohydrate transport and metabolism; and amino acid transport and metabolism were found to be more abundant in the rat gut microbiome (Fig. 7B). Metagenomic analysis based on the CAZy (Carbohydrate-Active enZymes) database showed that the functional classes of glycoside hydrolases (GHs), glycosyltransferases (GTs), and carbohydrate-binding modules (CBMs) were relatively abundant in the rat fecal microbiome, among the six CAZy functional modules (Fig. 7C).

Analysis of the differences in the relative abundance of functions

We continued to perform cluster analysis on the top 20 KEGG Orthology terms. At level 1, Cluster analysis indicated that, compared to the group C, the group PDN exhibited higher clustering in Metabolism, Genetic Information Processing, Human Diseases, Cellular Processes, Environmental Information Processing, and Organismal Systems (Fig. 8A). The level 2 categories-Carbohydrate Metabolism, Amino Acid Metabolism, Metabolism of Cofactors and Vitamins, Energy Metabolism, and Lipid Metabolism-were significantly higher in the group PDN compared to the group C (Fig. 8B). At level 3, cluster analysis showed that the group PDN exhibited higher levels in D-Alanine Metabolism, D-Glutamine and D-Glutamate Metabolism, Aminoacyl-tRNA Biosynthesis, Mismatch

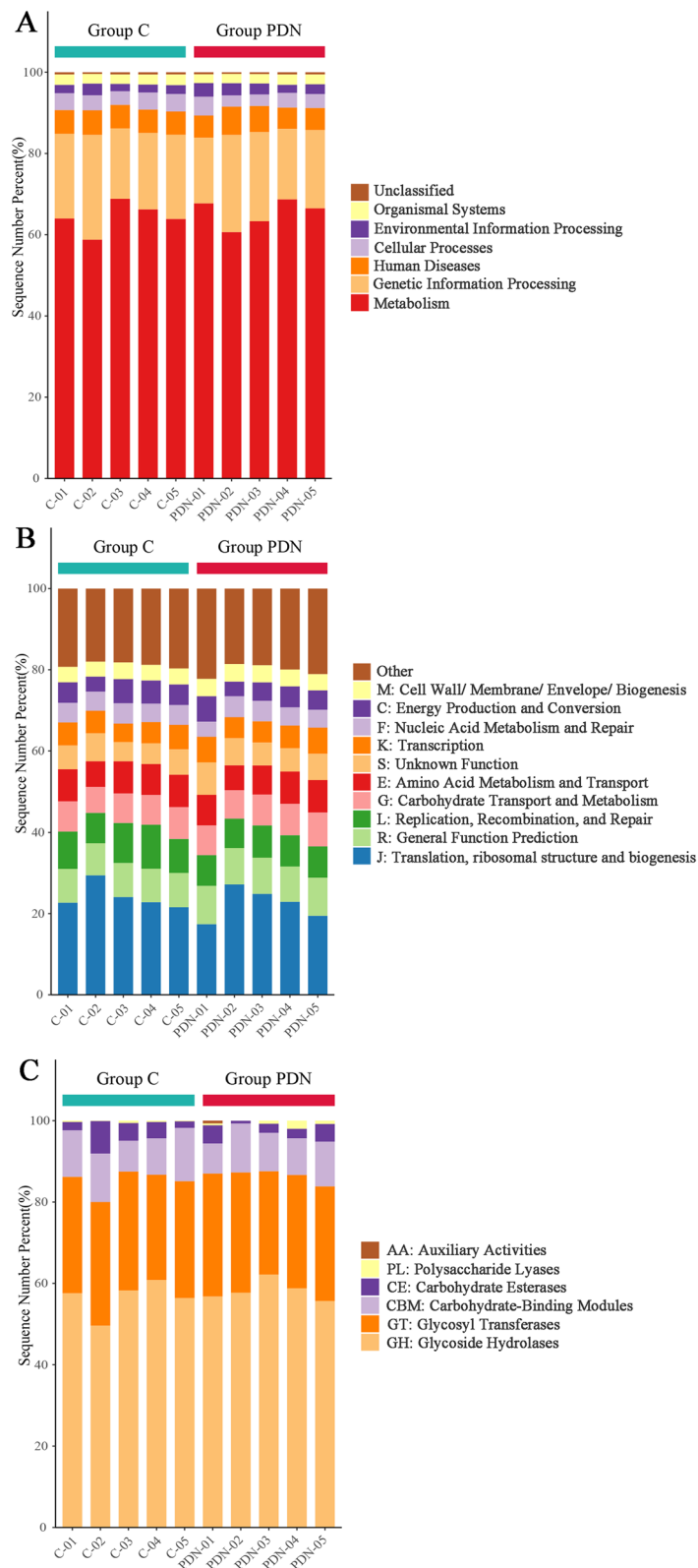


Fig. 7 Histogram of relative abundance of functional annotations on level 1. The results of KEGG, eggNOG, and CAZY are shown in order. **A**: Histogram of relative abundance of functional annotations in KEGG; **B**: Histogram of relative abundance of functional annotations in eggNOG; **C**: Histogram of relative abundance of functional annotations in CAZY. The vertical axis indicates the relative proportion of annotations to a functional class; the horizontal axis indicates the sample name; the functional class corresponding to each colour block is shown in the legend on the right

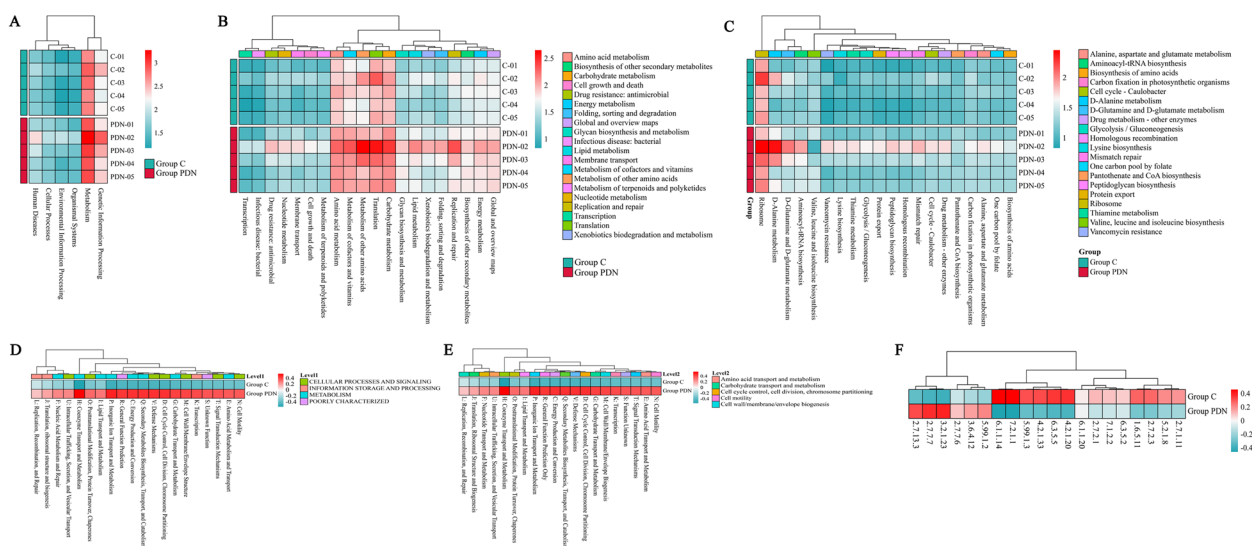


Fig. 8 Functional abundance clustering heat map. **A** Functional abundance clustering heat map in KEGG (level 1), **B** is for level 2, **C** is for level 3; **D** Functional abundance clustering heat map in eggnog (level 1), **E** is for level 2; **F**: Functional abundance clustering heat map in CAZy. Sample information is shown horizontally; functional annotation information is shown vertically; the clustering tree on the left side of the graph is the functional clustering tree; the values corresponding to the heat map in the middle are the Z-values obtained from normalising the relative abundance of the functions in each row

Repair, Cell Cycle-Caulobacter, Drug Metabolism—Other Enzymes, One Carbon Pool by Folate, Peptidoglycan Biosynthesis, Thiamine Metabolism, Glycolysis/Gluconeogenesis, Protein Export, Pantothenate and CoA Biosynthesis, Homologous Recombination, Vancomycin Resistance, and Lysine Biosynthesis compared to the group C (Fig. 8C). In metagenomic analysis based on the eggNOG database, functional classifications were categorized into two levels: level 1 and level 2. From Fig. 8D-E, we can observe that the microbial functions in the feces of rats in the group PDN are primarily enriched in the categories of cellular processes and signaling and metabolism. When further refined to more specific functional subclasses, the feces of rats in the group PDN show higher levels of Amino Acid Transport and Metabolism, Carbohydrate Transport and Metabolism, Cell Cycle Control, Cell Division, Chromosome Partitioning, Cell Motility, and Cell Wall/Membrane/Envelope Biogenesis compared to the group C. Functional annotation analysis based on the CAZy database revealed that the relative abundances of CEs, GTs, and PLs in the fecal microbiota of the group PDN were significantly higher than those in the group C, particularly for GHs and CBMs (Fig. 8F). Overall, these data further confirm that the metabolic characteristics of the intestinal microbiome in PDN rats have changed.

Discussion

Diabetic neuropathy is a prevalent complication among patients with diabetes, particularly those with T2DM. The high incidence of this complication is closely linked

to the age of onset and the underlying pathophysiological characteristics of diabetic patients. Previous studies have demonstrated that a reliable animal model of T2DM can be induced using a high-fat and high-sugar diet combined with intraperitoneal injections of a low dose of STZ (25 mg/kg), a method that has been widely adopted in related research [33]. However, it has been observed that estrogen can significantly affect blood glucose levels in female SD rats, leading to fluctuations and even a reduction in blood glucose following STZ injection [34]. Therefore, to mitigate this potential confounding factor, our study selected male SD rats as the experimental model. In our study, the metabolic changes observed in the group PDN, including persistent hyperglycemia, weight loss, and increased food and water consumption, are consistent with the classic symptoms of diabetes. The results from the IPGTT and ITT revealed that the group PDN exhibited impaired glycemic control and insulin resistance. This was evidenced by slower glucose clearance and significant blood glucose fluctuations following insulin administration, which mirrors the clinical manifestations of T2DM.

Systematic reviews and meta-analyses have highlighted that mechanical allodynia and thermal hyperalgesia are among the most prevalent and easily detectable symptoms in PDN. Furthermore, there is strong evidence supporting the link between mechanical allodynia and nerve damage in our model, we employed the Von Frey filament test and thermal pain apparatus, both of which

have been commonly used to evaluate these symptoms in the streptozotocin-induced PDN animal model [35, 36]. Mechanical allodynia, in particular, was a prominent feature in our study, consistent with previous findings [37]. To provide a more comprehensive and precise behavioral assessment of PDN, we suggest that future studies incorporate additional methodologies such as the pinprick test, pressure application measurement test, and Randall-Selitto test. These techniques would allow for a finer evaluation of changes in mechanical hyperalgesia, thus enriching the behavioral profile of PDN animal models and enhancing the overall understanding of the condition.

The observed reduction in MWT and TWL in group PDN one week after STZ injection suggests the early onset of pain hypersensitivity. This hyperalgesic state is consistent with known pathophysiological mechanisms underlying PDN, which include peripheral nerve fiber damage, mitochondrial dysfunction, and neuroinflammation [38, 39]. Notably, our results showed significant upregulation of pro-inflammatory cytokines TNF- α and IL-1 β in the spinal cord of group PDN. These cytokines are key mediators of neuroinflammation and play an essential role in sensitizing nociceptive neurons by enhancing excitatory synaptic transmission while simultaneously reducing inhibitory control in the dorsal horn of the spinal cord [40]. In addition to the central nervous system changes, we observed histological evidence of colonic mucosal damage and inflammatory infiltration in the group PDN. This finding suggests that the intestinal barrier function is compromised, which may contribute to systemic inflammation. Such inflammation could, in turn, exacerbate neuroinflammatory responses through the gut-spinal axis, further amplifying pain hypersensitivity. Taken together, these findings suggest that the pain hypersensitivity observed in PDN rats is not simply a behavioral phenotype but is deeply intertwined with inflammation-driven neuropathic processes. This supports the notion that systemic and central neuroinflammation are pivotal contributors to the pathogenesis of PDN. Our results align well with previous studies, which have indicated that hyperglycemia-induced oxidative stress and peripheral inflammation are significant drivers in the development of neuropathic pain. These insights reinforce the importance of targeting inflammation as a therapeutic approach in managing PDN. [41].

Histological analysis revealed significant structural damage in the colonic tissue of group PDN, characterized by epithelial cell shedding and extensive infiltration of inflammatory cells. These pathological changes indicate compromised intestinal barrier integrity, which may contribute to the development of "leaky gut syndrome." Concurrently, levels of pro-inflammatory

cytokines TNF- α and IL-1 β were significantly elevated in the spinal cord of group PDN, further supporting the hypothesis that dysbiosis of the gut microbiota may disrupt the intestinal barrier, thereby triggering spinal cord inflammation and exacerbating neuropathic pain. The spinal cord harbors a unique lymphatic-like clearance system known as the glymphatic system, which is responsible for the efficient removal of metabolic waste and inflammatory mediators from the central nervous system [42]. In our previous study, MRI imaging revealed a significant reduction in the uptake and clearance of exogenous contrast agents in the spinal cord of PDN rats, indicating impaired function of the spinal cord glymphatic system. Furthermore, we observed a marked increase in the activation of astrocytes in the spinal cord glymphatic system, with significant alterations in the expression and distribution of aquaporin-4 (AQP4), which may be a key factor in the development of pain [43]. Glial cells, as an essential component of the glymphatic system, play a crucial role in the onset and progression of PDN. Recent studies have shown that modulating glial cell activation can help restore normal pain perception [44]. Based on these findings, we propose that gut microbiota dysbiosis impairs intestinal barrier function, allowing pro-inflammatory mediators to enter the systemic circulation and accumulate in the spinal cord, where they provoke localized inflammatory responses. The excessive accumulation of these cytokines disrupts the expression and polarity of AQP4, further impairing glymphatic clearance and leading to inefficient removal of inflammatory mediators. This forms a vicious cycle of "inflammation accumulation–clearance impairment–inflammation amplification". Notably, anti-inflammatory agents such as ginkgolide B and liquiritin have been shown to significantly restore the expression and distribution of AQP4 in the spinal glymphatic system of PDN rats. This intervention partially recovers glymphatic system function and alleviates symptoms of neuropathic pain [14, 15]. In addition, astaxanthin has also been reported to relieve neuropathic pain by downregulating NMDA receptor activity and reducing lipopolysaccharide-induced oxidative stress in glial cells [45]. These findings suggest that suppressing the production of pro-inflammatory mediators and enhancing their clearance from the CNS may represent an effective therapeutic strategy for PDN. In summary, our results reveal a close association between gut microbiota dysbiosis and spinal cord inflammation, highlighting the critical role of the gut–spinal cord axis in the pathogenesis of PDN. This axis may serve as a promising target for future therapeutic interventions.

The gut microbiota, a crucial component of host metabolism and the immune system, has attracted significant attention in recent years. Numerous studies have

highlighted the close relationship between the diversity of the gut microbiome and the metabolic health of the host, especially in the context of metabolic diseases such as diabetes. [46]. Our microbial diversity analysis revealed no significant differences in α -diversity indices between group PDN and group C, suggesting similar species richness and evenness. However, β -diversity analysis revealed significant differences in the microbial community structure, implying that the composition of the microbiome is altered in the group PDN. This finding indicates that while overall diversity may remain similar, the specific makeup of the microbial communities is distinctly different between the groups. Previous studies have demonstrated that Bacillota and Bacteroidota dominate the mammalian gut microbiome. In this study, the gut microbiota composition of group PDN and group C showed similar distributions of major microbial phyla including Bacillota, Bacteroidota, Pseudomonadota, and Actinomycetota. Notably, the Bacillota/Bacteroidota ratio was lower in the group C (4.317) compared to the group PDN (19.254), indicating similar microbiota structural changes following a high-fat and high-sugar diet in group PDN. Of particular interest, we observed a significant decrease in the abundance of Spirochaetota in the group PDN. This phylum is known for its role in decomposing complex carbohydrates and proteins, which aids in nutrient absorption [47]. The reduced abundance of Spirochaetota in the group PDN suggests that the high-fat and high-sugar diet might inhibit the functions of this phylum, potentially affecting nutrient absorption and contributing to the pathophysiology of PDN.

Typically, diabetic patients exhibit gut microbial imbalance with an increase in harmful bacteria and a decrease in beneficial ones [48]. As a key probiotic, *Lactobacillus* not only maintains the acidic environment of the gut but also ferments undigested carbohydrates to produce SCFAs such as acetate, propionate, and butyrate, thereby promoting the restoration of microbial balance and playing a role in neuroprotection and the alleviation of neuroinflammation [49]. Numerous studies have shown that the abundance of *Lactobacillus* is significantly reduced in type 2 diabetes or PDN. Exogenous supplementation of *Lactobacillus* or modulation of its abundance through pharmacological interventions has been found to effectively delay disease progression [50, 51]. Further research reveals that *Lactobacillus* not only delays disease progression by regulating the MMP9 and NOTCH1 signaling pathways, but also improves the pathology of type 2 diabetes through various mechanisms, including the restoration of glucose homeostasis, repair of the intestinal barrier, and suppression of inflammation and oxidative stress [52, 53]. Interestingly, in some clinical patients or animal models, fecal samples from diabetic individuals

show an increased abundance of *Lactobacillus* [54, 55]. Moreover, studies have demonstrated that after treatment, the abundance of *Lactobacillus* in fecal samples of T2DM rats returns to normal levels [56].

Therefore, the observed increase in *Lactobacillus* in group PDN in this study may be considered an adaptive response to diabetic neuropathy. This inference is supported by LEfSe analysis, which showed a significant increase in *Lactobacillus*, *Lactobacillus acidophilus*, and *Lactobacillus paracasei* in the group PDN.

Collinsella, belonging to the Coriobacteriaceae family of the Actinobacteria phylum, is positively correlated with circulating insulin levels [57]. Accordingly, in populations with gestational diabetes and obesity—conditions often characterized by elevated insulin levels—the abundance of *Collinsella* is significantly increased [58, 59]. Interestingly, in obese patients with T2DM, weight reduction accompanied by decreased insulin levels leads to a corresponding decline in *Collinsella* abundance [58]. Furthermore, studies have demonstrated that insulin resistance is also associated with reduced levels of *Collinsella* [60]. In addition to its association with insulin metabolism, *Collinsella* abundance is closely linked to dietary fiber intake and SCFA metabolism [61]. Research has shown that low dietary fiber intake significantly increases the abundance of *Collinsella* in the gut microbiota of overweight and obese pregnant women. This may be due to a shift in the gut microbial community toward lactate fermentation under low-fiber conditions, which suppresses the growth of SCFA-producing bacteria [57]. In the present study, a reduced abundance of *Collinsella* was observed in the gut microbiota of group PDN. This phenomenon may primarily be attributed to the severe insulin resistance commonly present in group PDN. Additionally, group PDN often exhibit lower body weight, and as the disease progresses to neuropathy, insulin levels tend to decrease, which may further contribute to the reduced abundance of *Collinsella* in this group [62].

In the functional analysis based on the KEGG database, the group PDN displayed enhanced clustering in multiple metabolic pathways, particularly in metabolism, genetic information processing, and human disease categories. These findings suggest that the gut microbiome of the group PDN exhibits higher metabolic activity compared to the group C, which may be directly related to the metabolic dysregulation associated with diabetes. Studies have shown that long-term hyperglycemia and metabolic disorders can promote functional adjustments in the gut microbiome to metabolize carbohydrates and other nutrients more effectively, while potentially accompanying disruptions in intestinal barrier function, increasing the likelihood of bacterial permeation [63]. Therefore, the

observed enhancement in metabolic pathways may reflect the gut microbiome's adaptive response to the host's high glucose environment. Further analysis revealed significant enhancements in the group PDN in secondary and tertiary classifications such as carbohydrate metabolism and amino acid metabolism, consistent with our species difference analysis results. *Lactobacillus acidophilus* in the group PDN primarily involves carbohydrate metabolism, capable of producing lactic acid by fermenting lactose and other simple sugars [64]. Additionally, *L. acidophilus* can act synergistically with other probiotics like *Lactobacillus plantarum*, *Lactobacillus delbrueckii*, *Lactobacillus acidophilus*, *Lactobacillus rhamnosus*, and *Bifidobacterium bifidum*, playing an analgesic role by reducing cellular oxidative damage [65]. *Lactobacillus paragasseri*, a new species derived from *Lactobacillus gasseri*, primarily participates in the metabolism of lactose and other carbohydrates, influencing intestinal pH and the microbial environment through fermentation, exerting potential anti-anxiety and antidepressant effects [66]. With advances in taxonomy and DNA sequencing technologies, *Limosilactobacillus oris* has been found to influence intestinal development by modulating the gut microbial community [67]. *Clostridium disporicum* can ferment a variety of carbohydrates, potentially producing butyrate and other volatile fatty acids during this process [68]. Lastly, in the analyses of the EggNOG and CAZy databases, the group PDN showed an increase in the abundance of functional groups related to translation, replication and repair, carbohydrate transport and metabolism, and amino acid transport and metabolism, with significant increases in the relative abundance of glycosyl hydrolases, glycosyltransferases, and carbohydrate-binding modules. These results further support the enhanced capability of the gut microbiome in adapting to a high-sugar environment in the degradation and utilization of carbohydrates and amino acids. These functional changes may also contribute to the inflammatory milieu observed in group PDN, further linking microbial dysbiosis to neuropathic pain.

Currently, the mechanisms by which gut microbiota influence the onset and progression of PDN remain incompletely understood. Dysbiosis of the gut microbiota often leads to increased intestinal permeability, commonly referred to as "leaky gut." This condition permits bacterial endotoxins such as lipopolysaccharide and other inflammatory mediators to enter the bloodstream, triggering systemic inflammatory responses [69]. In diabetic patients, persistent hyperglycemia activates the immune system and induces chronic inflammation, which is closely associated with neural damage [70]. For instance, proinflammatory cytokines such as TNF- α , IL-1 β , and

IL-6 can promote neuronal apoptosis and inhibit axonal regeneration, thereby exacerbating pain perception [71]. Moreover, following peripheral nerve injury, the expression of the *Kcna2* gene is downregulated, leading to reduced voltage-gated potassium currents and increased neuronal excitability, which contribute to the development of neuropathic pain. These represent potential pathophysiological mechanisms underlying PDN [72]. Secondly, SCFAs, metabolic products generated by the gut microbiota through the fermentation of dietary fibers, mainly include acetate, propionate, and butyrate. SCFAs can inhibit inflammatory responses by activating G-protein-coupled receptors, such as GPR41 and GPR43 [73], and alleviate inflammation induced by diabetes by reducing the release of inflammatory factors from macrophages and other immune cells, thereby protecting neurons [74]. Notably, targeting G protein-coupled receptors not only reduces the excessive activation of primary neurons, effectively relieving pain, but also avoids adverse effects on the central nervous system [75]. Additionally, SCFAs regulate pain perception by modulating the sensitivity of nociceptive neurons and affecting the activation and polarization of microglia [76, 77]. Butyrate, in particular, has been recognized to promote the synthesis of neurotrophic factors, such as brain-derived neurotrophic factor, supporting neuronal survival and regeneration, and improving neural function [78]. Lastly, the gut-brain axis describes the bidirectional communication pathway between the gut and the central nervous system, involving interactions among the neural, endocrine, and immune systems. Via the vagus nerve in the gut directly connected to the brain, intestinal information can be directly transmitted to the central nervous system. This neural connection plays a significant role in regulating emotions, pain, and immune responses [79, 80]. The dysbiosis of the gut microbiota under diabetic conditions leads to the activation of macrophages and lymphocytes, which are increasingly recognized for their roles in neural damage and pain perception [81, 82]. These findings further support the concept of the gut microbiota as a potential therapeutic target for diabetic neuropathy, possibly through the regulation of the microbial community to alleviate related symptoms.

Regulating the gut microbiota presents potential prospects for the prevention and treatment of PDN. Future research should focus on how interventions in the gut microbiota can influence the progression of PDN and its underlying mechanisms. Existing experimental studies have demonstrated the potential to reduce inflammation and β -cell death in type 2 diabetes induced by streptozotocin through the administration of various probiotics or prebiotics to animal models [83, 84]. Furthermore,

therapeutic approaches combining pharmacological treatments with interventions in the gut microbiome have shown superior effects in diabetic rats [85, 86]. Probiotics, as non-pharmacological interventions, are particularly noted for their excellent safety profile and broad adaptability. Thus, assessing the effects of different probiotics in conjunction with pharmacological treatments on the improvement of PDN symptoms, exploring the associations between changes in gut microbiota diversity and pain perception, inflammatory responses, and neural function recovery, constitutes an important research direction. Additionally, diet significantly affects the composition and function of the gut microbiota. Studies have shown that optimizing dietary structure, such as increasing dietary fiber intake and reducing the consumption of high-fat foods, can promote the growth of beneficial bacteria, thereby improving the gut microbial balance [87, 88]. Dietary patterns rich in antioxidants, such as the Mediterranean diet, may offer protective effects against neuropathy in diabetic patients [89]. Therefore, future research should focus on the impact of different dietary patterns on diabetic neuropathy and explore suitable dietary intervention strategies for diabetic patients. A comprehensive treatment strategy combining probiotics and dietary interventions may provide an effective method to combat diabetic neuropathy.

The design of this experiment has several limitations. Firstly, although the experiment initially included 25 rats, only 10 (group C: 5, group PDN: 5) provided data for analysis. This limited sample size may reduce the power of statistical analyses, decrease the ability to detect subtle effects or differences, and could increase the risk of false negatives or false positives, thereby affecting the accurate interpretation of the relationship between changes in the gut microbiota and PDN. While the sample size in this study is relatively small, we took several steps to ensure the robustness of our results. First, we employed rigorous experimental protocols and utilized appropriate statistical methods to minimize the impact of the limited sample size. Furthermore, to minimize statistical bias arising from the sample size, we strictly controlled the experimental procedures. All animals were kept in the same environment, fed with the same diet, and all procedures were performed by a trained and experienced personnel. Additionally, non-parametric statistical tests and multiple comparison corrections (such as FDR) were applied in the data analysis to ensure the reliability of the statistical inferences. Secondly, the observation period was 15 weeks, which, while possibly sufficient to observe some chronic effects of PDN, is inadequate to capture the dynamic changes in insulin levels or the gut microbiome over time for such a chronic disease. Therefore, extending the observation period could better aid in understanding

the interactions between the gut microbiome and PDN over time. Third, the standard SD rat model used in the study may not fully simulate the complex pathophysiological characteristics of human diabetes patients, thus potentially limiting the translatability of the results from this model to humans. Finally, the different dietary regimens used during the modeling phase for the group C and the group PDN (standard diet vs. high-fat, high-sugar diet) might influence the composition of the gut microbiome. Although all rats were switched to a standard diet after the successful establishment of the PDN, the dietary differences in the earlier stages could still directly affect the microbiome composition, potentially confounding the assessment of the PDN group's impact on the microbiome. Furthermore, while we monitored the food intake of the rats during the early stages and balanced the food intake between the two groups based on the monitoring results, no dynamic monitoring was conducted in the later stages to adjust food intake, which could still influence the experimental outcomes.

To address the limitations highlighted in this study, future research should consider several improvements. First, increasing the sample size will enhance statistical power and provide more reliable results. Extending the observation period will also allow for a more thorough understanding of the long-term effects of PDN on gut microbiota and metabolic changes. To improve the relevance to human disease, future studies could explore alternative animal models that more closely mimic the pathophysiology of human diabetic neuropathy, such as transgenic rats. Additionally, standardizing the dietary regimens across the entire experimental period and continuously monitoring food intake, body weight, and metabolic markers will help control for confounding factors. Finally, adopting multi-omics approaches, including metagenomics, metabolomics, and proteomics, will provide deeper insights into the complex interactions between gut microbiota and PDN, facilitating a better understanding of the underlying mechanisms and informing the development of more effective therapeutic strategies.

Conclusions

In summary, this study reveals significant alterations in the intestinal microbiota of PDN rats, accompanied by compromised intestinal barrier function and elevated inflammation. These findings highlight the critical role of gut dysbiosis in PDN pathogenesis and suggest that restoring microbial homeostasis may represent a promising approach for managing PDN. Further studies are warranted to explore the underlying mechanisms and therapeutic potential of the gut microbiome in diabetic.

Abbreviations

T2DM	Type 2 diabetes mellitus
PDN	Painful diabetic neuropathy
SCFAs	Short-chain fatty acids
STZ	Streptozotocin
IPGTT	Intraperitoneal glucose tolerance test
ITT	Insulin tolerance test
MWT	Mechanical withdrawal threshold
TWL	Thermal withdrawal latency
HE	Hematoxylin–eosin
PCoA	Principal coordinates analysis
NMDS	Non-metric multidimensional scaling
LEFSe	Linear Discriminant Analysis Effect Size
LDA	Linear Discriminant Analysis
EggNOG	Evolutionary Genealogy of Genes: Non-supervised Orthologous Groups
CAZy	Carbohydrate-Active enZYmes
GHs	Glycoside hydrolases
GTs	Glycosyltransferases
CBMs	Carbohydrate-binding modules

Acknowledgements

We sincerely grateful to the Hepatobiliary Institute and Anesthesia Laboratory of North Sichuan Medical College for providing us with the experimental platform.

Authors' contributions

SJ and JL designed the experiment. SJ, HM and YS conducted animal experiment, collected samples, analyzed the data, drafted the paper, and extracted the DNA from stool samples. YL and ZM aided in the ELISA experiments and pathological staining procedures. SJ, HM and YS provided substantive edits to the manuscript. All authors read through the manuscript prior to its submission. All authors read and approved the final manuscript.

Funding

This research was supported by the Nanchong Science and Technology Bureau Municipal School Cooperation Project (22SXQT0125) and the School-level Key Scientific Research Project of North Sichuan Medical College (CBY22-ZDA09).

Data availability

The data collected in the present study were properly analyzed and summarized in the Results section. Metagenomic raw sequencing data have been deposited in NCBI Sequence Read Archive (SRA) (accession numbers for NCBI: BioProject: PRJNA1192041). the following data identifiers correspond to the datasets used in our study: Group C (GC1, GC2, GC3, GC4, GC5); Group PDN (GP1, GP2, GP3, GP4, GP5). Raw data can be accessed here: <http://www.ncbi.nlm.nih.gov/bioproject/1192041>.

Declarations

Ethics approval and consent to participate

This experiment involved SD rats provided by the Experimental Animal Center of North Sichuan Medical College. All experimental procedures were approved by the Institutional Ethics Committee of North Sichuan Medical College (authorization number: 2024[071]). All procedures adhered strictly to the ARRIVE guidelines for the Care and Use of Experimental Animals.

Consent for publication

Not applicable.

Competing interests

The authors declare no competing interests.

Received: 1 December 2024 Accepted: 30 April 2025

Published online: 08 May 2025

References

- Zimmet PZ. Diabetes and its drivers: the largest epidemic in human history? *Clin Diabetes Endocrinol.* 2017;3:1.
- Zimmet P, Alberti KG, Magliano DJ, Bennett PH. Diabetes mellitus statistics on prevalence and mortality: facts and fallacies. *Nat Rev Endocrinol.* 2016;12(10):616–22.
- Callaghan BC, Price RS, Chen KS, Feldman EL. The importance of rare subtypes in diagnosis and treatment of peripheral neuropathy: a review. *JAMA Neurol.* 2015;72(12):1510–8.
- Callaghan BC, Cheng HT, Stables CL, Smith AL, Feldman EL. Diabetic neuropathy: clinical manifestations and current treatments. *Lancet Neurol.* 2012;11(6):521–34.
- Gylfadottir SS, Christensen DH, Nicolaisen SK, Andersen H, Callaghan BC, Itani M, Khan KS, Kristensen AG, Nielsen JS, Sindrup SH, et al. Diabetic polyneuropathy and pain, prevalence, and patient characteristics: a cross-sectional questionnaire study of 5,514 patients with recently diagnosed type 2 diabetes. *Pain.* 2020;161(3):574–83.
- Griebeler ML, Morey-Vargas OL, Brito JP, Tsapas A, Wang Z, Carranza Leon BG, Phung OJ, Montori VM, Murad MH. Pharmacologic interventions for painful diabetic neuropathy: An umbrella systematic review and comparative effectiveness network meta-analysis. *Ann Intern Med.* 2014;161(9):639–49.
- Feldman EL, Callaghan BC, Pop-Busui R, Zochodne DW, Wright DE, Bennett DL, Bril V, Russell JW, Viswanathan V. Diabetic neuropathy. *Nat Rev Dis Primers.* 2019;5(1):42.
- Lin Q, Li K, Chen Y, Xie J, Wu C, Cui C, Deng B. Oxidative stress in diabetic peripheral neuropathy: pathway and mechanism-based treatment. *Mol Neurobiol.* 2023;60(8):4574–94.
- Ma S, Nakamura Y, Hisaoka-Nakashima K, Morioka N. Blockade of receptor for advanced glycation end-products with azeliragon ameliorates streptozotocin-induced diabetic neuropathy. *Neurochem Int.* 2023;163: 105470.
- Hu Y, Chen C, Liang Z, Liu T, Hu X, Wang G, Hu J, Xie X, Liu Z. Compound qiyang granules alleviates diabetic peripheral neuropathy by inhibiting endoplasmic reticulum stress and apoptosis. *Mol Med (Cambridge, Mass).* 2023;29(1):98.
- Tiwari V, He SQ, Huang Q, Liang L, Yang F, Chen Z, Tiwari V, Fujita W, Devi LA, Dong X, et al. Activation of μ - δ opioid receptor heteromers inhibits neuropathic pain behavior in rodents. *Pain.* 2020;161(4):842–55.
- Gadepalli A, Ummadisetty O, Akhilesh, Chouhan D, Yadav KE, Tiwari V. Peripheral mu-opioid receptor activation by dermorphin [D-Arg2, Lys4] (1-4) amide alleviates behavioral and neurobiological aberrations in rat model of chemotherapy-induced neuropathic pain. *Neurotherapeutics.* 2024;21(1):e00302.
- Bidve P, Prajapati N, Kalia K, Tekede R, Tiwari V. Emerging role of nanomedicine in the treatment of neuropathic pain. *J Drug Target.* 2020;28(1):11–22.
- Li J, Jia S, Song Y, Xu W, Lin J. Ginkgolide B can alleviate spinal cord lymphatic system dysfunction and provide neuroprotection in painful diabetic neuropathy rats by inhibiting matrix metalloproteinase-9. *Neuropharmacology.* 2024;250: 109907.
- Jia SY, Yin WQ, Xu WM, Li J, Yan W, Lin JY. Liquiritin ameliorates painful diabetic neuropathy in SD rats by inhibiting NLRP3-MMP-9-mediated reversal of aquaporin-4 polarity in the glymphatic system. *Front Pharmacol.* 2024;15: 1436146.
- Kant R, Chandra L, Verma V, Nain P, Bello D, Patel S, Ala S, Chandra R, Antony MA. Gut microbiota interactions with anti-diabetic medications and pathogenesis of type 2 diabetes mellitus. *World J Methodol.* 2022;12(4):246–57.
- Huang W, Lin Z, Sun A, Deng J, Manyande A, Xiang H, Zhao GF, Hong Q. The role of gut microbiota in diabetic peripheral neuropathy rats with cognitive dysfunction. *Front Microbiol.* 2023;14: 1156591.
- Montandon SA, Jornayvaz FR. Effects of antidiabetic drugs on gut microbiota composition. *Genes.* 2017;8(10):250.
- Wang Y, Ye X, Ding D, Lu Y. Characteristics of the intestinal flora in patients with peripheral neuropathy associated with type 2 diabetes. *J Int Med Res.* 2020;48(9): 300060520936806.
- Sabico S, Al-Mashharawi A, Al-Daghri NM, Wani K, Amer OE, Hussain DS, Ahmed Ansari MG, Masoud MS, Alokail MS, McTernan PG. Effects of a 6-month multi-strain probiotics supplementation in endotoxemic, inflammatory and cardiometabolic status of T2DM patients: a

- randomized, double-blind, placebo-controlled trial. *Clin Nutr (Edinburgh, Scotland)*. 2019;38(4):1561–9.
21. Defaye M, Gervason S, Altier C, Berthon JY, Ardid D, Filaire E, Carvalho FA. Microbiota: a novel regulator of pain. *J Neural Transm (Vienna, Austria : 1996)*. 2020;127(4):445–65.
 22. Yang NJ, Chiu IM. Bacterial signaling to the nervous system through toxins and metabolites. *J Mol Biol*. 2017;429(5):587–605.
 23. Gou Y, Liu B, Cheng M, Yamada T, Iida T, Wang S, Banno R, Koike T. d-Allulose ameliorates skeletal muscle insulin resistance in high-fat diet-fed rats. *Molecules (Basel, Switzerland)*. 2021;26(20):6310.
 24. Saande CJ, Steffes MA, Webb JL, Valentine RJ, Rowling MJ, Schalinke KL. Whole egg consumption impairs insulin sensitivity in a rat model of obesity and type 2 diabetes. *Curr Dev Nutr*. 2019;3(4):nzz015.
 25. Nirogi R, Goura V, Shanmuganathan D, Jayarajan P, Abraham R. Comparison of manual and automated filaments for evaluation of neuropathic pain behavior in rats. *J Pharmacol Toxicol Methods*. 2012;66(1):8–13.
 26. Hargreaves K, Dubner R, Brown F, Flores C, Joris J. A new and sensitive method for measuring thermal nociception in cutaneous hyperalgesia. *Pain*. 1988;32(1):77–88.
 27. Langmead B, Salzberg SL. Fast gapped-read alignment with Bowtie 2. *Nat Methods*. 2012;9(4):357–9.
 28. Mandal S, Van Treuren W, White RA, Eggesbø M, Knight R, Peddada SD. Analysis of composition of microbiomes: a novel method for studying microbial composition. *Microb Ecol Health Dis*. 2015;26:27663.
 29. Franzosa EA, Mclver LJ, Rahnavard G, Thompson LR, Schirmer M, Weingart G, Lipson KS, Knight R, Caporaso JG, Segata N, et al. Species-level functional profiling of metagenomes and metatranscriptomes. *Nat Methods*. 2018;15(11):962–8.
 30. Chen L, Jiang Q, Lu H, Jiang C, Hu W, Yu S, Xiang X, Tan CP, Feng Y, Zhang J, et al. Antidiabetic effect of sciadonic acid on type 2 diabetic mice through activating the PI3K-AKT signaling pathway and altering intestinal flora. *Front Nutr*. 2022;9: 1053348.
 31. Qi B, Ren D, Li T, Niu P, Zhang X, Yang X, Xiao J. Fu brick tea manages HFD/STZ-induced type 2 diabetes by regulating the gut microbiota and activating the IRS1/PI3K/Akt signaling pathway. *J Agric Food Chem*. 2022;70(27):8274–87.
 32. Xie J, Song W, Liang X, Zhang Q, Shi Y, Liu W, Shi X. Jinmaitong ameliorates diabetic peripheral neuropathy in streptozotocin-induced diabetic rats by modulating gut microbiota and neuregulin 1. *Aging*. 2020;12(17):17436–58.
 33. Akinlade OM, Owoyeye BV, Soladoye AO. Streptozotocin-induced type 1 and 2 diabetes in rodents: a model for studying diabetic cardiac autonomic neuropathy. *Afr Health Sci*. 2021;21(2):719–27.
 34. Paschou SA, Papanas N. Type 2 diabetes mellitus and menopausal hormone therapy: an update. *Diabetes Ther*. 2019;10(6):2313–20.
 35. Sierra-Silvestre E, Somerville M, Bisset L, Coppieters MW. Altered pain processing in patients with type 1 and 2 diabetes: systematic review and meta-analysis of pain detection thresholds and pain modulation mechanisms. *BMJ Open Diabetes Res Care*. 2020;8(1):1–9.
 36. Lolignier S, Eijkelkamp N, Wood JN. Mechanical allodynia. *Pflugers Arch*. 2015;467(1):133–9.
 37. Bodman MA, Dreyer MA, Varacallo MA: Diabetic peripheral neuropathy. In: StatPearls. Treasure Island (FL) ineligible companies. Disclosure: Mark Dreyer declares no relevant financial relationships with ineligible companies. Disclosure: Matthew Varacallo declares no relevant financial relationships with ineligible companies.: StatPearls Publishing Copyright © 2025, StatPearls Publishing LLC.; 2025.
 38. Garcia-Nicas E, Laird JMA, Cervero F. Vasodilatation in hyperalgesic rat skin evoked by stimulation of afferent A beta-fibers: further evidence for a role of dorsal root reflexes in allodynia. *Pain*. 2001;94(3):283–91.
 39. Traub RJ. Spinal modulation of the induction of central sensitization. *Brain Res*. 1997;778(1):34–42.
 40. Boakye PA, Tang SJ, Smith PA. Mediators of neuropathic pain; focus on spinal microglia, CSF-1, BDNF, CCL21, TNF- α , Wnt ligands, and interleukin 1 β . *Front Pain Res (Lausanne, Switzerland)*. 2021;2: 698157.
 41. Calcutt NA. Diabetic neuropathy and neuropathic pain: a (con)fusion of pathogenic mechanisms? *Pain*. 2020;161(Suppl 1):S65–s86.
 42. Liu S, Lam MA, Sial A, Hemley SJ, Bilston LE, Stoodley MA. Fluid outflow in the rat spinal cord: the role of perivascular and paravascular pathways. *Fluids Barriers CNS*. 2018;15(1):13.
 43. Wang GQ, Wang FX, He YN, Lin JY. Plasticity of the spinal glymphatic system in male SD rats with painful diabetic neuropathy induced by type 2 diabetes mellitus. *J Neurosci Res*. 2022;100(10):1908–20.
 44. Tiwari V, Guan Y, Raja SN. Modulating the delicate glial-neuronal interactions in neuropathic pain: promises and potential caveats. *Neurosci Biobehav Rev*. 2014;45:19–27.
 45. Sharma K, Sharma D, Sharma M, Sharma N, Bidve P, Prajapati N, Kalia K, Tiwari V. Astaxanthin ameliorates behavioral and biochemical alterations in in-vitro and in-vivo model of neuropathic pain. *Neurosci Lett*. 2018;674:162–70.
 46. Lau WL, Tran T, Rhee CM, Kalantar-Zadeh K, Vaziri ND. Diabetes and the gut microbiome. *Semin Nephrol*. 2021;41(2):104–13.
 47. Hernández R, Chaib De Mares M, Jimenez H, Reyes A, Caro-Quintero A. Functional and phylogenetic characterization of bacteria in bovine rumen using fractionation of ruminal fluid. *Front Microbiol*. 2022;13:813002.
 48. Yang X, Che T, Tian S, Zhang Y, Zheng Y, Zhang Y, Zhang X, Wu Z. A living microecological hydrogel with microbiota remodeling and immune reinstatement for diabetic wound healing. *Adv Healthcare Mater*. 2024;13(23): e2400856.
 49. Xiong RG, Zhou DD, Wu SX, Huang SY, Saimaiti A, Yang ZJ, Shang A, Zhao CN, Gan RY, Li HB. Health benefits and side effects of short-chain fatty acids. *Foods (Basel, Switzerland)*. 2022;11(18):2863.
 50. Tawulie D, Jin L, Shang X, Li Y, Sun L, Xie H, Zhao J, Liao J, Zhu Z, Cui H, et al. Jiang-Tang-San-Huang pill alleviates type 2 diabetes mellitus through modulating the gut microbiota and bile acids metabolism. *Phytomedicine*. 2023;113:154733.
 51. Jiang Y, Yang J, Wei M, Shou J, Shen S, Yu Z, Zhang Z, Cai J, Lyu Y, Yang D, et al. Probiotics alleviate painful diabetic neuropathy by modulating the microbiota-gut-nerve axis in rats. *J Neuroinflammation*. 2025;22(1):30.
 52. Chen S, Han P, Zhang Q, Liu P, Liu J, Zhao L, Guo L, Li J. *Lactobacillus brevis* alleviates the progress of hepatocellular carcinoma and type 2 diabetes in mice model via interplay of gut microflora, bile acid and NOTCH 1 signaling. *Front Immunol*. 2023;14: 1179014.
 53. Song H, Xue H, Zhang Z, Wang J, Li A, Zhang J, Luo P, Zhan M, Zhou X, Chen L, et al. Amelioration of type 2 diabetes using four strains of lactobacillus probiotics: effects on gut microbiota reconstitution-mediated regulation of glucose homeostasis, inflammation, and oxidative stress in mice. *J Agric Food Chem*. 2023;71(51):20801–14.
 54. Gaike AH, Paul D, Bhute S, Dhotre DP, Pande P, Upadhyaya S, Reddy Y, Sampath R, Ghosh D, Chandraprabha D, et al. The gut microbial diversity of newly diagnosed diabetics but not of prediabetics is significantly different from that of healthy nondiabetics. *mSystems*. 2020;5(2):1–17.
 55. Chen PC, Chien YW, Yang SC. The alteration of gut microbiota in newly diagnosed type 2 diabetic patients. *Nutrition (Burbank, Los Angeles County, Calif)*. 2019;63–64:51–6.
 56. Zhao Z, Chen Y, Li X, Zhu L, Wang X, Li L, Sun H, Han X, Li J. Myricetin relieves the symptoms of type 2 diabetes mice and regulates intestinal microflora. *Biomed Pharmacother = Biomed Pharmacother*. 2022;153: 113530.
 57. Gomez-Arango LF, Barrett HL, Wilkinson SA, Callaway LK, McIntyre HD, Morrison M, Dekker Nitert M. Low dietary fiber intake increases *Collinsella* abundance in the gut microbiota of overweight and obese pregnant women. *Gut microbes*. 2018;9(3):189–201.
 58. Frost F, Stork LJ, Kacprowski T, Gärtner S, Rühlemann M, Bang C, Franke A, Völker U, Aghdassi AA, Steveling A, et al. A structured weight loss program increases gut microbiota phylogenetic diversity and reduces levels of *Collinsella* in obese type 2 diabetics: a pilot study. *PLoS ONE*. 2019;14(7): e0219489.
 59. Zhong S, Yang B, Liu Y, Dai W, Li G, Yang J, Yang A, Wang Y, Wang M, Xu C, et al. Dynamic changes of gut microbiota between the first and second trimester for women with gestational diabetes mellitus and their correlations with BMI: a nested cohort study in China. *Front Microbiol*. 2024;15: 1467414.
 60. Livantsova EN, Leonov GE, Starodubova AV, Varaeva YR, Vatlin AA, Koshechkin SI, Korotkova TN, Nikityuk DB. Diet and the gut microbiome as determinants modulating metabolic outcomes in young obese adults. *Biomedicine*. 2024;12(7):1601.
 61. Medawar E, Haange SB, Rolle-Kampczyk U, Engelmann B, Dietrich A, Thieleking R, Wiegank C, Fries C, Horstmann A, Villringer A, et al. Gut

- microbiota link dietary fiber intake and short-chain fatty acid metabolism with eating behavior. *Transl Psychiatry*. 2021;11(1):500.
62. Nauck MA. Unraveling the science of incretin biology. *Am J Med*. 2009;122(6 Suppl):S3-s10.
 63. Hsu CL, Schnabl B. The gut-liver axis and gut microbiota in health and liver disease. *Nat Rev Microbiol*. 2023;21(11):719–33.
 64. Goh YJ, Klaenhammer TR. A functional glycogen biosynthesis pathway in *Lactobacillus acidophilus*: expression and analysis of the *glg* operon. *Mol Microbiol*. 2013;89(6):1187–200.
 65. Shabani M, Hasanpour E, Mohammadifar M, Bahmani F, Talaei SA, Aghighi F. Evaluating the effects of probiotic supplementation on neuropathic pain and oxidative stress factors in an animal model of chronic constriction injury of the sciatic nerve. *Basic and clinical neuroscience*. 2023;14(3):375–84.
 66. Hashikawa-Hobara N, Otsuka A, Okujima C, Hashikawa N. *Lactobacillus paragasseri* OLL2809 improves depression-like behavior and increases beneficial gut microbes in mice. *Front Neurosci*. 2022;16: 918953.
 67. Lyu L, Zhou X, Zhang M, Liu L, Liu T, Niu H, Wu Y, Liang C, Han X, Zhang L. *Lactobacillus* derived from breast milk facilitates intestinal development in IUGR rats. *J Appl Microbiol*. 2022;133(2):503–14.
 68. Wang B, Lei S, Li Q, Luo Y. Production of lactulose from lactose using a novel cellobiose 2-epimerase from *Clostridium disporicum*. *Enzyme Microb Technol*. 2024;179: 110466.
 69. Usuda H, Okamoto T, Wada K. Leaky gut: effect of dietary fiber and fats on microbiome and intestinal barrier. *Int J Mol Sci*. 2021;22(14):7613.
 70. Cheng YC, Chu LW, Chen JY, Hsieh SL, Chang YC, Dai ZK, Wu BN. Loganin attenuates high glucose-induced schwann cells pyroptosis by inhibiting ROS generation and NLRP3 inflammasome activation. *Cells*. 2020;9(9):1948.
 71. Hua T, Yang M, Song H, Kong E, Deng M, Li Y, Li J, Liu Z, Fu H, Wang Y, et al. Huc-MSCs-derived exosomes attenuate inflammatory pain by regulating microglia pyroptosis and autophagy via the miR-146a-5p/TRAF6 axis. *Journal of nanobiotechnology*. 2022;20(1):324.
 72. Zhao X, Tang Z, Zhang H, Atianjoh FE, Zhao JY, Liang L, Wang W, Guan X, Kao SC, Tiwari V, et al. A long noncoding RNA contributes to neuropathic pain by silencing *Kcna2* in primary afferent neurons. *Nat Neurosci*. 2013;16(8):1024–31.
 73. Kim MH, Kang SG, Park JH, Yanagisawa M, Kim CH. Short-chain fatty acids activate GPR41 and GPR43 on intestinal epithelial cells to promote inflammatory responses in mice. *Gastroenterology*. 2013;145(2):396–406. e391–310.
 74. Park J, Kim M, Kang SG, Jannasch AH, Cooper B, Patterson J, Kim CH. Short-chain fatty acids induce both effector and regulatory T cells by suppression of histone deacetylases and regulation of the mTOR-S6K pathway. *Mucosal Immunol*. 2015;8(1):80–93.
 75. Uniyal A, Tiwari V, Tsukamoto T, Dong X, Guan Y, Raja SN. Targeting sensory neuron GPCRs for peripheral neuropathic pain. *Trends Pharmacol Sci*. 2023;44(12):1009–27.
 76. Zhou F, Wang X, Han B, Tang X, Liu R, Ji Q, Zhou Z, Zhang L. Short-chain fatty acids contribute to neuropathic pain via regulating microglia activation and polarization. *Mol Pain*. 2021;17: 1744806921996520.
 77. Lanza M, Filippone A, Casili G, Giuffrè L, Scuderi SA, Paterniti I, Campolo M, Cuzzocrea S, Esposito E. Supplementation with SCFAs re-establishes microbiota composition and attenuates hyperalgesia and pain in a mouse model of NTG-induced migraine. *Int J Mol Sci*. 2022;23(9):4847.
 78. Li Y, Liu A, Chen K, Li L, Zhang X, Zou F, Zhang X, Meng X. Sodium butyrate alleviates lead-induced neuroinflammation and improves cognitive and memory impairment through the ACS52/H3K9ac/BDNF pathway. *Environ Int*. 2024;184: 108479.
 79. Wang Q, Yang Q, Liu X. The microbiota-gut-brain axis and neurodevelopmental disorders. *Protein Cell*. 2023;14(10):762–75.
 80. Guo R, Chen LH, Xing C, Liu T. Pain regulation by gut microbiota: molecular mechanisms and therapeutic potential. *Br J Anaesth*. 2019;123(5):637–54.
 81. Carlos D, Pérez MM, Leite JA, Rocha FA, Martins LMS, Pereira CA, Fraga-Silva TFC, Pucci TA, Ramos SG, Câmara NOS, et al. NOD2 deficiency promotes intestinal CD4+ T lymphocyte imbalance, meta-inflammation, and aggravates type 2 diabetes in murine model. *Front Immunol*. 2020;11: 1265.
 82. Li H, Liu S, Chen H, Zhou L, Chen B, Wang M, Zhang D, Han TL, Zhang H. Gut dysbiosis contributes to SCFAs reduction-associated adipose tissue macrophage polarization in gestational diabetes mellitus. *Life Sci*. 2024;350: 122744.
 83. Hsieh PS, Ho HH, Tsao SP, Hsieh SH, Lin WY, Chen JF, Kuo YW, Tsai SY, Huang HY. Multi-strain probiotic supplement attenuates streptozotocin-induced type-2 diabetes by reducing inflammation and β -cell death in rats. *PLoS ONE*. 2021;16(6): e0251646.
 84. Alharbi HF, Algonaiman R, Barakat H. Ameliorative and antioxidative potential of *Lactobacillus plantarum*-fermented oat (*Avena sativa*) and fermented oat supplemented with sidr honey against streptozotocin-induced type 2 diabetes in rats. *Antioxidants (Basel, Switzerland)*. 2022;11(6):1122.
 85. Yang Q, Cai X, Zhu Y, Hu Z, Wei Y, Dang Q, Zhang Y, Zhao X, Jiang X, Yu H. Oat β -glucan supplementation pre- and during pregnancy alleviates fetal intestinal immunity development damaged by gestational diabetes in rats. *Food Funct*. 2023;14(18):8453–66.
 86. Yan H, Lu J, Wang Y, Gu W, Yang X, Yu J. Intake of total saponins and polysaccharides from *Polygonatum kingianum* affects the gut microbiota in diabetic rats. *Phytomedicine*. 2017;26:45–54.
 87. Wang K, Wang Y, Chen S, Gu J, Ni Y. Insoluble and soluble dietary fibers from Kiwifruit (*Actinidia deliciosa*) modify gut microbiota to alleviate high-fat diet and streptozotocin-induced TYPE 2 diabetes in rats. *Nutrients*. 2022;14(16):3369.
 88. Huang Y, Ashaolu TJ, Olatunji OJ. Micronized dietary okara fiber: characterization, antioxidant, antihyperglycemic, antihyperlipidemic, and pancreato-protective effects in high fat diet/streptozotocin-induced diabetes mellitus. *ACS Omega*. 2022;7(23):19764–74.
 89. Khemayanto H, Shi B. Role of Mediterranean diet in prevention and management of type 2 diabetes. *Chin Med J*. 2014;127(20):3651–6.

Publisher's Note

Springer Nature remains neutral with regard to jurisdictional claims in published maps and institutional affiliations.